QUBEKit: Automating the Derivation of Force Field Parameters from Quantum Mechanics

Joshua T. Horton,[†] Alice E. A. Allen,[‡] Leela S. Dodda,[¶] and Daniel J. Cole[*,†]

[†]*School of Natural and Environmental Sciences, Newcastle University, Newcastle upon Tyne NE1 7RU, United Kingdom*

[‡]*TCM Group, Cavendish Laboratory, 19 JJ Thomson Avenue, Cambridge CB3 0HE, United Kingdom*

[¶]*Department of Chemistry, Yale University, New Haven, Connecticut 06520-8107, United States*

E-mail: *daniel.cole@ncl.ac.uk

Abstract

Modern molecular mechanics force fields are widely used for modelling the dynamics and interactions of small organic molecules using libraries of transferable force field parameters. However, for molecules outside the training set, the parameters are potentially inaccurate and it may be preferable to derive molecule-specific parameters. Here we present an intuitive parameter derivation toolkit, QUBEKit (QUantum mechanical BEspoke Kit), which enables the automated generation of system-specific small molecule force field parameters directly from quantum mechanics. QUBEKit is written in python and combines bond, angle, torsion, charge and Lennard-Jones parameter derivation methodologies alongside a method for deriving the positions and charges of off-center virtual sites from the partitioned quantum mechanical electron density. As a proof of concept, we have re-derived a complete set of parameters for 109 small organic molecules, and assessed the accuracy by comparing computed liquid properties with experiment. QUBEKit gives competitive results when compared to standard transferable force fields, with mean unsigned errors of 0.024 g/cm^3, 0.79 kcal/mol and 1.17 kcal/mol for the liquid density, heat of vaporization and free energy of hydration respectively. This indicates that the derived parameters are suitable for molecular modeling applications, including computer-aided drug design.

Introduction

Complex biological processes such as protein-ligand binding,[1,2] enzyme catalysis, and protein folding are often best understood when studied at the atomic scale which has driven an increase in the popularity of molecular mechanics (MM) and computational experiments. The ability of MM to model systems ranging in sizes from thousands to millions of atoms makes it indispensable across a wide range of sciences from biology to materials physics. The key to the general success of MM stems from the force field (FF) and its functional form, which allow the approximate description of the potential energy surface of a system as a simple function of its geometry.[3]

Transferable FFs such as GAFF (general AMBER FF),[4] CGENFF (CHARMM general FF)[5] and OPLS-AA[6] are designed to be used in conjunction with their respective highly optimized and benchmarked biological FF counterpart. They are primarily used in simulating drug-like components of systems in, for example, computer-aided drug design, and give non-expert users the ability to parametrize highly diverse expanses of chemical space at very little computational cost. The requirement that a FF be transferable stems from two key points, 1) the parametrization process is a complex and error-prone task that is daunting to the inexperienced user, and 2) an attempt to accurately parametrize all of chemical space would be inconceivable. It is therefore generally assumed that as long as a wide selection of chemical space is covered in the parametrization set then these results can readily be applied to new molecules. Each of the general FFs use libraries composed of thousands of pre-tabulated parameters,[7] intensively fit to experimental and QM data for a set of small molecules that make up their training set. The parametrization goal of these particular FFs focusses on recreating experimental data concerning the condensed phase thermodynamic properties of small organic molecules, such as liquid densities, heats of vaporization and free energies of hydration.[5] This parametrization philosophy follows sound logic as these properties describe the FF's ability to accurately characterize the non-bonded interactions that are also key in protein-ligand binding events. Furthermore, the accuracy and applicability of transferable FFs are aided by efforts such as ForceBalance[8] and the Open Force Field Consortium,[9] which aim to expand the areas of chemical space that can be automatically parametrized via well-documented protocols.

However, no matter how much effort is put into parameterizing small molecules against experimental data, the assumption of transferability remains. That is, the assumption that parameters that are optimal for small organic molecules are also suitable for larger molecules, such as drug-like compounds or even biomolecules. It is well-established that charges polarize in response to their environment, for example the presence of electron donating or withdrawing groups.[10] Indeed, users of transferable FFs typically derive system-specific charges to account for this polarization, either from semi-empirical or QM calculations.[11–13] Moreover, it is becoming increasingly apparent that van der Waals parameters themselves show interesting environment-dependent responses.[14,15] Accounting for changes in van der Waals parameters with changes in FF charges, or the atomic environment, is beyond the scope of most transferable FF protocols.

A fundamentally different approach to FF parameterization is to instead derive the FF directly from quantum mechanical (QM) simulations of the molecule under study. The potential of using such calculations to develop intermolecular FF potentials for small molecules has long been recognized.[16–20] Here, instead of assuming transferability, the user is able to derive parameters that are specific to their system using a range of automated protocols. Perhaps the most conceptually straightforward approach to QM-based intermolecular force field derivation is to generate many configurations of the system, and fit force field parameters to reproduce the QM energies and/or forces.[21–24] This approach may be applied to quite large molecules using the fragmentation reconstruction method, but extensive sampling of the intermolecular potential energy surface is required for accurate parameter derivation.[25] Alternatively, *ab initio* force fields have been developed that break down the QM interaction energy into physically motivated components using intermolecular perturbation theory.[26–28] These methods incoporate important electronic effects, allow for systematic improvement of intermolecular energies, and can potentially be derived from a very small number of high level *ab initio* calculations.[29] However, compared with more widely-used transferable force fields, *ab initio* force fields generally employ a more complex functional form, which is slower to evaluate, and due to the cost of the underlying QM calculation the majority of applications are to relatively small system sizes. In this regard, Grimme's quantum mechanically derived force field (QMDFF) has several advantages. It takes as input only the QM equilibrium structure, partial charges, Hessian matrix, covalent bond orders and semi-empirical torsion scans, and outputs a full molecule-specific force field.[30] The QM input can be relatively cheap, it is has been applied to molecules comprising more than 100 atoms, and can even be used to model bond dissociation and metals. However, it again uses a more complex functional form compared to standard, transferable force fields, and its accuracy in the condensed phase and the feasibility of extending the approach to heterogeneous problems, such as protein-ligand binding, are yet to be established.

Our goal in this paper is to describe a QM-derived force field that has the potential to be easily extended to the types of problems usually reserved for standard, transferable force fields, such as host-guest binding in solution,[31] simulation of biomolecular assemblies,[32] and computer-aided drug design.[33] To set up a transferable FF for a small molecule, a user typically performs a QM geometry optimization to fit atomic charges (typically to the QM electrostatic potential), and maybe performs torsional scans for key dihedrals. In order to be competitive with transferable FFs, our FF derivation technique should i) allow users to derive all system-specific bonded and non-bonded FF parameters from these two simple QM input calculations, ii) scale up to relatively large system sizes (e.g. 50–100 atoms), iii) provide parameters suitable for use in mixed simulations (e.g. for the molecule in a solvent or in host-guest simulations), iv) retain the simple functional form of transferable FFs for implementation in the majority of classical MD codes and for use in free energy calculations, v) retain or improve on the accuracy of transferable FFs for modelling of condensed phase properties (and hence implicitly account for many-body effects). That is, we aim to remove any FF limitations associated with parameter transferability, and instead adopt a transferable FF derivation methodology akin to the semi-empirical models routinely used for charge derivation.

Towards this goal, we have investigated and developed a range of methods for deriving FF parameters directly from QM calculations with minimal experimental fitting. One of the techniques employed in this study is the modified Seminario method,[34,35] which enables the derivation of bond stretching and angle bending force constants directly from the QM Hessian matrix computed at the optimized geometry. Deriving bonded FF parameters from QM data,[36–39] and in particular from the Hessian matrix[35,40–45] is a well-established concept. Our recent adaptation of the original Seminario method[35] yields high quality parameters without relying on iterative fitting of the MM Hessian matrix, which avoids interdependency between force field parameters.[34] In particular, the modified Seminario method has been shown to give parameters that are able to reproduce QM vibrational frequencies with an average error of 49 cm^{-1} for a test set of 70 molecules, which is slightly lower than that achieved by OPLS-AA (59 cm^{-1}) and competitive with methods that rely on iterative fitting of the MM Hessian matrix.[30,44,46] The second of the methods employed here is atoms-in-molecule (AIM) analysis, which provides a means to partition the QM molecular electron density amongst the constituent atoms, and hence assign atom-centered partial charges, even for systems comprising many thousands of atoms.[47,48] Furthermore, the partitioned atomic electron densities can also be used in conjunction with the Tkatchenko-Scheffler (TS) relations[14] to calculate all of the L-J parameters for a molecule. This method of using QM-derived non-bonded parameters has been shown to perform well in recreating liquid densities and thermodynamic properties when applied to a test set of 40 organic molecules.[48] Collectively these methods form the basis of the QUantum mechanical BEspoke (QUBE) FF.[49]

Here, we present QUBEKit, a software toolkit designed to help users derive QUBE FF parameters in an intuitive and consistent way that minimizes parameter interdependency. This first iteration combines previously benchmarked QM derivation methods for non-bonded, bond stretching, angle bending and torsion parameters, using the same functional form as the OPLS-AA FF, and is freely available to the community via our Github page (https://github.com/cole-group/QUBEKit). Continuing a previous study that benchmarked the accuracy of the atoms-in-molecule non-bonded parameter derivation method, we re-derive parameters for a larger test set comprising over 100 small organic molecules using QUBEKit in a proof-of-concept workflow. We also expand upon the original non-bonded parameter derivation process by adding new fitting parameters that allow the derivation of FF terms for compounds containing bromine, as well as implementing a method for the derivation of off-center virtual site positions and charges directly from the QM electron density to model anisotropic electron densities. Combining these techniques we show through the use of the standard FF metrics described that the level of accuracy achievable with a QUBE FF is comparable to that of widely-used general transferable FFs. In this way, we provide the community with a tool for checking and refining parameter sets assigned through chemical similarity, and a starting point for FF improvements through optimization of the derivation protocols.

Theoretical background

FFs are traditionally described using bond-stretching, angle-bending, dihedral rotation, electrostatic and L-J contributions, as exemplified by the OPLS functional form:

$$\begin{gathered}U = \sum_{Bonds} \frac{k_r}{2}(r - r_o)^2 + \sum_{Angles} \frac{k_\theta}{2}(\theta - \theta_o)^2 \\ + \sum_{Dihedrals} \left[\frac{V_1}{2}(1 + cos(\phi)) + \frac{V_2}{2}(1 - cos(2\phi)) + \frac{V_3}{2}(1 + cos(3\phi)) + \frac{V_4}{2}(1 - cos(4\phi)) \right] \\ + \sum_{Pairs} \frac{q_i q_j}{r_{ij}} + \left(\frac{A_{ij}}{r_{ij}^{12}} - \frac{B_{ij}}{r_{ij}^{6}} \right)\end{gathered} \tag{1}$$

The bond-stretching and angle-bending contributions require estimates of the force constants k_r and k_θ respectively as well as reference bond lengths (r_o) and angles (θ_o). The dihedral term is described as a four component cosine series with four corresponding parameters V_1, V_2, V_3, V_4, where ϕ is the torsion angle of the dihedral being described. The OPLS FF also employs an improper dihedral term through the same potential form, using only a V_2 parameter. The final term accounts for all non-bonded interactions between pairs of atoms seperated by a distance r_{ij}. The standard Coulomb potential is used to calculate the interaction between two charges q_i and q_j. Finally, the short-range repulsion and longer-range attractive van der Waals interactions are described using the L-J 12-6 potential. Here $\mathrm{A}_{ij} = 4\epsilon_{ij}\sigma_{ij}^{12}$ and $\mathrm{B}_{ij} = 4\epsilon_{ij}\sigma_{ij}^{6}$ where the ϵ and σ values of the L-J potential govern the energy well depth and minimum energy separation distance respectively. In the OPLS FF, non-bonded interactions are excluded for atoms separated by one or two covalent bonds, and are scaled by a factor of 0.5 for those separated by three bonds. The same set of non-bonded parameters are used to compute inter- and intra-molecular components of the FF.

A complete set of parameters for any molecule described by this FF functional form requires the derivation of all the parameters of eq 1. Traditionally each term has its own parameter fitting protocol and order that varies between FFs. Our derivation scheme follows this idea, breaking the problem down into individual tasks that have an order of best practice. In particular, we begin by calculating the stretching and bending terms, followed by non-bonded, and finally the dihedral parameters. Next, we shall discuss the motivation behind the derivation and optimization methods combined in QUBEKit.

Bond and Angle Parameters

For each bond and angle in our molecule, we require a force constant and equilibrium value in order to describe the internal energy contribution associated with the vibrational motion. It has been noted that, to describe all of the basic atom type combinations in GAFF, some 20,000 angle parameters would be required.[4] Such large parameter libraries are commonplace with OPLS3 containing 15,236 angle-bending parameters, with a continuing effort to expand this list as new chemistries are encountered.[7] To generate these parameters, general FFs have to use a wide range of reference data combining experiment and QM. QM data actually already play a role in the derivation of the majority of the transferable parameters in these FFs due to the lack of experimental data available for unique chemical species and the ease of generating accurate QM data on-the-fly. While many of the equilibrium terms are collected from x-ray crystallography and NMR studies of small molecules, some have to be determined from QM predicted minimum energy structures.[4–7] Force constants are then manually fit in an iterative process which aims to recreate the QM vibrational frequencies using an initial guess for the other required parameters as described in the development of CGENFF[5] and AMBER.[4] While this method is effective, it does create interdependencies in the FF parameters as the force constants are dependent on the rest of the original parameter set, meaning that ideally all parameters should be continually updated in a self-consistent fashion until convergence is reached.[5]

Instead, we have adopted the modified Seminario method for deriving bond and angle force field parameters. The standard Seminario method derives force constants directly from the QM Hessian matrix[35] and has been incorporated into specialized FF fitting tools for metal complexes such as the VFFDT plugin,[50] or in the MCPB.py[51] program which is part of AmberTools. This method estimates force constants by projecting the decomposed forces felt by an atom due to the displacement of a neighboring atom onto their mutual bond vector.[35] However, this method results in undesirably stiff force constants due to the double counting of angle bending contributions in larger molecules.[34] The modified method, however, accounts for an atom's chemical environment and has been shown to recreate QM vibrational frequencies with a low average error of 6.3% across all vibrational modes for a wide range of molecules.[34] The ability to accurately derive the bonded parameters directly from the QM Hessian matrix without the need for initial parameter guesses simplifies the procedure for non-expert users by removing sources of human error and also speeds up the process making it suitable for automation. We shall also show that the derived force constants retain a low percentage error in recreating QM vibrational frequencies when combined with the rest of the QUBE FF.

Non-Bonded Parameters

The non-bonded interactions incorporate multiple QM effects, such as electrostatics, induction, dispersion and exchange-repulsion, through effective non-bonded Coulombic and L-J interactions. In fixed point charge models there are many methods to derive partial charges from high-level QM calculations using a mixture of population analysis techniques, but ultimately no unique solution. While *ab initio* calculations yield high-quality charges they are often disregarded as being too computationally expensive and are substituted by a variety of semi-empirical QM based methods. These methods allow the rapid assignment of charges and are heavily parametrized in order to reproduce charges observed at higher levels of theory. For example, GAFF employs Mulliken charges produced from semi-empirical Austin Model 1 (AM1) calculations[52] that are then subject to bond charge corrections (BCC) to better recreate experimental hydration free energies.[11,12] The resulting electrostatic potential is then comparable to that calculated at the HF/6-31G* level which was used to parameterize the AMBER restrained electrostatic potential (RESP) charges.[4] OPLS-AA, on the other hand, uses Cramer-Truhlar CM1A[13] charges, and recently also included an AM1-BCC inspired localized BCC version of the OPLS-AA/CM1A FF that is available through the LigParGen server.[53–55] It should also be noted that, as these semi-empirical QM calculations are performed in vacuum, they have to be modified to include polarization effects to make them suitable for condensed phase modelling. This is often performed via the inclusion of the BCC mentioned in the case of GAFF and OPLS, and/or in the form of charge scaling factors all of which are only used on neutral molecules.

On the other hand, CGENFF relies heavily on *ab initio* calculations. CGENFF I charges can be first assigned by a similarity search through a library of parametrized fragments or can be derived using MP2/6-31G(d) Merz-Kollman charges.[5] With either starting guess, the charges are subsequently optimized by fitting to QM-calculated scaled interaction energies at the HF/6-31G(d) level between the molecule and water in a variety of conformations. Again we note the choice of low-level theory, this an artefact from the initial derivation of the CHARMM additive FF, to ensure any new parameters are compatible with the biological CHARMM terms. Importantly this means the overall charge description is compatible between systems that require a mix of transferable and biological FFs.

Computational cost is also kept to a minimum in standard transferable FFs by assigning the L-J parameters from a library of pre-fit parameters. This has become standard practice across transferable FFs, with OPLS3 containing 124 different atom types so far, and many general FFs borrowing terms from their biological counterparts.[4,7] The L-J potential parameters are often tuned to accurately recreate experimental liquid properties.[5,6,39,56] While this technique works very well for atoms covered in the original parameterization, more atom types often have to be introduced to account for new chemical environments. During the optimization of the GAMMP/GAFF-LJ* parameters, for example, it was found that for a test set of 430 compounds the 41 standard atom types of GAFF were restricting the maximum achievable accuracy of the FF. The performance was then substantially increased with the addition of 11 new atom types, reducing the average unsigned relative error in the heat of vaporization from 17.9% to 5.9%.[39] Clearly increasing the number of atom types will help increase the overall accuracy of a FF as new exceptions to current atom types arise. Logically this implies that system-specific FF parameters have the potential to lead to an overall more accurate FF.

The QUBE FF follows this QM-based philosophy by deriving both L-J parameters and AIM charges from a single ground state QM electron density. The AIM partitioning method divides the total molecular electron density ($n(\mathbf{r})$) into approximately spherical, uniform overlapping atomic densities ($n_i(\mathbf{r})$) via:

$$n_i(\mathbf{r}) = \frac{w_i(\mathbf{r})}{\sum_k w_k(\mathbf{r})} n(\mathbf{r}) \tag{2}$$

The weighting factor $w_i(\mathbf{r})$ is determined by the choice of AIM partitioning method, in our case the density derived electrostatic and chemical charges (DDEC)[57,58] scheme is employed. This method iteratively optimizes the weighting factor to resemble the spherical average of $n_i(\mathbf{r})$ and the density of a similar reference ion using a mixture of iterative Hirshfeld (IH) and iterative Stockholder atoms (ISA).[48,57] The charges are then found by integrating the atomic electron density over all space:

$$q_i = z_i - N_i = z_i - \int n_i(\mathbf{r}) d^3\mathbf{r} \tag{3}$$

Where N_i is the number of electrons associated with atom i and z_i is the nuclear charge. The electron density is calculated as the direct solution of the inhomogeneous Poisson equation in a medium with a dielectric constant $\epsilon = 4$.[48] It was found that "half-polarizing" the molecule with a low dielectric constant resulted in non-bonded terms that are suitable for condensed phase modelling. Including polarization in this manner allows us to avoid parametrizing any BCC or charge scaling factors as employed by CGENFF, OPLS/CM1A and OPLS/CM5.[59]

Additionally, the QUBE FF employs the TS method to derive the A_{ij} and B_{ij} terms of the FF in equation 1 by rescaling reference free atom data, proportionally to AIM electron densities.[14] The dispersion coefficient B_i is estimated as:

$$B_i = \left(\frac{V_i^{AIM}}{V_i^{free}} \right)^2 B_i^{free} \tag{4}$$

The atomic volume is readily calculated from the same AIM partitioned electron density as used in charge assignment via:

$$V_i^{AIM} = \int r^3 n_i(\mathbf{r}) d^3\mathbf{r} \tag{5}$$

The B_i^{free} coefficients are computed using time-dependent density functional theory (TDDFT) calculations on free atoms in vaccum.[60] V_i^{free} is the reference volume of the atom calculated using the MP4(SDQ)/aug-cc-pVQZ method in Gaussian 09[61] and the chargemol code[62] for each of the elements in our model (Table S1). To ensure that the dispersion and repulsion coefficients result in a minimum in the L-J potential close to the van der Waals radius of the atom, it can be shown that the A_i coefficient can be approximated by:

$$A_i = \frac{1}{2} B_i (2R_i^{AIM})^6 \tag{6}$$

Here we found the AIM effective radius R^{AIM} of each atom by rescaling the reference free atom radius using the TS method:

$$R_i^{AIM} = \left(\frac{V_i^{AIM}}{V_i^{free}} \right)^{1/3} R_i^{free} \tag{7}$$

The only parameters in our model that are fit to experiment are the eight free atom radii (R_i^{free}), one for each of the elements studied so far (H, C, N, O, F, S, Cl, Br). This version sees the addition of a bromine parameter that was fit in the same spirit as the rest, that is empirically tuning the free atom radii to recreate liquid properties of a selection of bromine-containing molecules. The dependence of computed liquid properties on the R_i^{free} parameter of bromine is displayed in Table S2. A full description of the non-bonded parameter derivation methods can be found in Ref. 48.

Anisotropy

While atom-centered point charges provide a good representation of the QM electrostatic potential (ESP) if the partitioned atomic electron density is spherical, in many cases this simple representation is inadequate.[48] This situation occurs when there is significant anisotropy in the underlying electron distribution, and is common in molecules containing nitrogen, sulfur or halogens.[63] Here, to model electron anisotropy, we employ off-center, "virtual" sites, which have been shown to be competitive with the use of more computationally expensive higher-order multipole electrostatics.[64] Virtual sites are commonly used in water models, such as TIP4P,[65] and various force fields for modelling lone pairs and σ-holes,[66] but the positions and charges of the virtual sites require fitting to experiment. On the other hand, it has recently been shown that virtual site positions may be derived directly from localized QM molecular orbitals,[67,68] but currently the magnitudes of the charges are derived by fitting to the molecular dipole moment, which may be problematic for extension to larger molecules that contain multiple sites. In keeping with our goal of avoiding fitting FF parameters to experiment and developing methods that scale to biological molecules, we proposed a method that relied on the dipole and quadrupole moments of the partitioned atomic electron density, to optimize the charges and locations of virtual sites.[48] However, the method employed did not consistently converge and resulted in a large number of off-center point charges. Modifications were required to correct these issues and improve the usability of the method in an automated high-throughput scenario.

Here, we propose a method for the derivation of virtual site positions and charges directly from the QM electron density in which the virtual sites are positioned so as to reproduce as closely as possible the QM ESP of the partitioned atomic electron density. By determining the virtual site parameters only using atomic properties, the method scales trivially to macromolecules such as proteins. In order to reduce the search space we limit the virtual site positions to those dictated by the symmetry of the atom's bonding environment. Together these improvements allow us to define virtual sites that improve the electrostatic properties of the simulated molecule in an automated manner.

The QM ESP (Φ_i^{ref}) is calculated from the partitioned atomic electron density ($\mathrm{n}_i(\mathbf{r})$). This is advantageous as the method may be applied equally well to both surface and buried atoms. The ESP is taken at a series of points on sets of spheres with radii between $1.4 - 2.0$ times the van der Waals radius of the atom. The error $F(\Phi, \Phi^{ref})$ is given by:

$$F(\Phi, \Phi^{ref}) = \sum_{i=1}^{M} \frac{|\Phi_i - \Phi_i^{ref}|}{M} \tag{8}$$

where M is the number of sampling points. The MM ESP (Φ_i) is calculated as:

$$\Phi_i = \sum_{j=1}^{N} \frac{q_j}{4\pi\epsilon_0 r_{ij}} \tag{9}$$

where N is the number of sites on an atom, r_{ij} is the distance from the site to the sampling point and q_j is the charge on site j. An additional threshold parameter (F_{thresh}) was required to distinguish between atoms that required extra sites and those that did not. Above this threshold the anisotropy method is used, below the threshold, no off-center charges are added. As well as this, extra charges are only added when there is a reduction in error which is controlled by a second parameter (F_{change}).

One Additional Off Center Charge

For atoms with ESP error above the threshold, we begin by attempting to model the anisotropy using a single off-center charge. The vectors for one additional off-center point charge that preserve symmetry are shown in Fig. 1. The vector direction is governed by the number of atoms bonded to the atom exhibiting anisotropy:

1. *One bond.* The atom A (which exhibits anisotropy) has one neighbor, atom B. The vector along which the extra charge is positioned is $\mathbf{r_1} = \lambda_1 \mathbf{r_{AB}}$, where $\mathbf{r_{AB}}$ is a vector between atom A and atom B and λ_1 is to be determined.

2. *Two bond.* The atom A has two neighbors, atoms B and C. The vector for the extra charge is $\mathbf{r_1} = \lambda_1(\mathbf{r_{AB}} + \mathbf{r_{AC}})$, which is along the bisector of the two bond vectors.

3. *Three bond.* The atom A has three neighbors, atoms B, C and D. The vector for the extra charge is $\mathbf{r_1} = \lambda_1(\mathbf{r_{AB}} - \mathbf{r_{AC}}) \times (\mathbf{r_{AD}} - \mathbf{r_{AC}})$, which makes an equal angle with all three bond vectors.

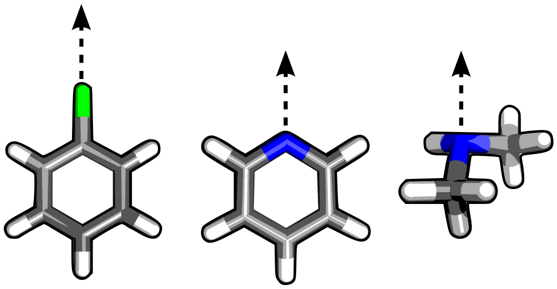

Figure 1: The directions along which off-center point charges are placed for an atom with one, two or three bonds.

After the vector is assigned, the optimal position along the vector and the charge of the off-center point is determined. This is carried out using a grid search of parameters to find the values which best recreate the QM ESP. Assigning a symmetry-derived search direction reduces the number of variables that need to be optimized from four (the x, y, z coordinates and the charge) to two (the distance along the vector and the charge). This simplification is particularly important when multiple off-center point charges are added, as described in the following section. The atom-centered point charge is assigned a value such that the net charge of the atom is unchanged. The method is summarized with a flowchart in Figure S1.

Multiple Off-Center Charges

In Ref. 48, it was often necessary to add more than one off-center point charge to recreate the anisotropy seen in the QM ESP. Therefore, our approach was extended to add multiple charges. Again, the method depends on the number of atoms bonded to the atom exhibiting anisotropy:

1. *One bond.* A second off-center charge is placed along the same vector, $\mathbf{r_2} = \lambda_2 \mathbf{r_{AB}}$.

2. *Two bonds.* If two extra point charges are used, the original vector is a line of symmetry. The two charges are then placed in the same plane as the vectors that point from the atom to the neighboring atoms, $\mathbf{r_{1,2}} = \lambda_{\|}(\mathbf{r_{AB}} + \mathbf{r_{AC}}) \pm \lambda_{\perp}(\mathbf{r_{AB}} + \mathbf{r_{AC}}) \times (\mathbf{r_{AB}} \times \mathbf{r_{AC}})$, or perpendicular to this plane, $\mathbf{r_{1,2}} = \lambda_{\|}(\mathbf{r_{AB}} + \mathbf{r_{AC}}) \pm \lambda_{\perp}(\mathbf{r_{AB}} \times \mathbf{r_{AC}})$. An example is shown in Fig. 2. A third extra charge can also be added and is placed along the bisector $\mathbf{r_3} = \lambda_3(\mathbf{r_{AB}} + \mathbf{r_{AC}})$.

3. *Three bonds.* A second off-center charge is placed along the same vector, $\mathbf{r_2} = \lambda_2(\mathbf{r_{AB}} - \mathbf{r_{AC}}) \times (\mathbf{r_{AD}} - \mathbf{r_{AC}})$. An exception is made for primary amine groups with the second off-center charge placed along the bisector of the NH_2 angle $\mathbf{r_2} = \lambda_2(\mathbf{r_{NH_1}} + \mathbf{r_{NH_2}})$. This is necessary as the regions between the nitrogen and hydrogen atoms exhibit anisotropy in ESP.

A disadvantage of using the partitioned electron density to calculate the QM ESP is that it includes regions that are not accessible during MM simulations, such as between bonds. This is the case for the amine group and results in other regions of the QM ESP not being adequately reproduced. The addition of an off-center site between the nitrogen and hydrogen atoms helps to overcome this issue.

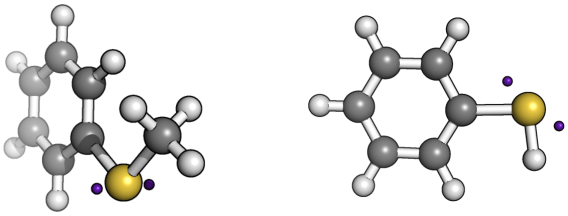

Figure 2: An example of off-center charge placement for the case (left) perpendicular to the plane of the bond vectors or (right) in the plane of the bond vectors.

Torsional Parameters

The final stage in the fitting procedure is the optimization of torsional parameters. Torsional rotation is an important factor controlling the conformational preference of a molecule due to its association with QM stereoelectronic effects, and the parameters are therefore often a target for re-optimization.[7,46,69–74] In this work, we follow a standard procedure of fitting the parameters to minimize the difference between MM and QM constrained one dimensional torsional scans. In particular, we aim to fit the four V_n parameters of the OPLS FF torsion potential shown in eq 1 by automating the scheme outlined in Ref. 70 into QUBEKit with some additional considerations. The steepest descent algorithm is employed to find the torsional parameters that minimize the regularized Boltzmann weighted error function:

$$\Omega = \sqrt{\frac{\sum_{i=1}^{n}(\Delta E^{i}_{MM} - \Delta E^{i}_{QM})^2 e^{-\Delta E^{i}_{QM}/k_B T}}{n}} + \lambda \sum_{torsions} \sum_{j=1}^{4} |V_j^{ref} - V_j| \qquad (10)$$

where k_B is the Boltzmann constant, T is a temperature weighting factor, n is the number of sampling points and V_j^{ref} is a reference torsional parameter. ΔE_{QM} and ΔE_{MM} are the QM and MM optimized energies at each sampled torsional angle relative to the lowest QM or MM energy. MM scans allow all other degrees of freedom to optimize, and so the structures are similar but not identical to the QM optimized structures. Overfitting is often a concern at this point in the fitting process. Here, we introduce a regularization function controlled by a variable parameter λ, which constrains the fitted torsional parameters to be close to the reference values, V_j^{ref}. In this work, V_j^{ref} were taken from the OPLS force field, but could also be set to zero.[75] It is also important to note that it is not possible to always perfectly recreate the entire QM potential energy surface hence users should concentrate on relatively low energy regions as these are most likely to be sampled during room temperature simulations. The weighting temperature T can be adjusted to preferentially weight the low-energy regions of the QM potential energy surface.

In molecules containing multiple flexible dihedral angles, it was found that torsional parameters were best fit in an order that started with rotations that would involve the movement of the fewest number of atoms. For example, a long chain molecule with no repeated dihedral types would be best fit by starting at the ends and working inwards. Larger molecules could also be fragmented during fitting to reduce the computational cost of the fitting procedure. It should also be noted that we do not derive any improper torsion parameters in this workflow, instead taking them from the OPLS-AA FF.

Computational Implementation

QUBEKit has been designed as a python command line toolkit with simple, intuitive commands allowing the user to perform three main tasks: 1) writing QM input files for atoms-in-molecule, Hessian matrix and torsional scan calculations, 2) derivation of bond, angle, torsion and non-bonded MM parameters from the results of the QM calculations, and 3) the output of the parameters in widely-used MM topology and force field files. The only required inputs are the molecule's structure and some initial reference parameters, which are included in a BOSS z-matrix, which is freely available via the LigParGen web server (http://jorgensenresearch.com/ligpargen/).[53–55] LigParGen provides a straightforward interface for generation of z-matrices. Users can draw, enter the SMILES string or upload a PDB file of a molecule (up 200 atoms), which is then automatically converted to a z-matrix. The use of internal coordinates makes defining and choosing the dihedral angle to be optimized conceptually straightforward.

In this first version of QUBEKit, QM calculations are currently performed using the Gaussian09[61] and ONETEP[76] software packages. QUBEKit interfaces with the BOSS[77] molecular simulation package to perform all MM tasks, including torsional fitting and vibrational mode analysis, and incorporates code from the modified Seminario method[34] to calculate the bond and angle parameters. Future support for additional open source MM and QM software packages is planned. The derived parameters can be written in a variety of MM package formats such as BOSS/MCPRO style (z-matrices, .sb and .par structural and force field files), OpenMM .xml files, and GROMACS .gro and .top files. A full description of the workflow (Figure S3) used in this project with a list of commands can be found on our Github page (https://github.com/cole-group/QUBEKit) alongside a tutorial.

Computational Methods

Quantum Mechanical Calculations

All Gaussian09 input files were prepared using QUBEKit, which takes PDB files and the corresponding BOSS/MCPRO style z-matrices generated using the LigParGen web server as input. All optimization routines and frequency calculations used for the bond stretching and angle bending terms were performed with the ωB97X-D[78] functional using the 6-311++G(d,p) basis set and a vibrational scaling factor of 0.957.[34] Users of QUBEKit are free to choose their own QM methods based on required accuracy and computational expense. For comparison, Tables S7 and S8 show the derived bond and angle parameters of N-butyl-1-butanamine computed using ωB97X-D/6-311++G(d,p) and MP2/6-311++G(d,p). Torsional constrained optimizations were performed in Gaussian09[61] with the same functional and basis set so as to be consistent with the other bonded terms. The torsional scan optimizations were performed in 15° increments from 0° to 360°. The majority of the dihedral parameter fitting was done using no Boltzmann weighting (corresponding to T=∞) and regularization against OPLS reference values was applied with $\lambda = 0.1$. This was only changed in rare cases where it was particularly difficult to recreate the QM energy landscape, in which case $\lambda = 0$ and $T = 2000K$ were used as previously suggested.[70]

Ground-state electron density calculations for non-bonded parameter derivation were performed using the linear-scaling DFT code ONETEP.[76] Four nonorthogonal generalized Wannier functions (NGWFs), with radii of 10 Bohr, were used for all atoms with the exception of hydrogen, which used one. NGWFs were expanded in a periodic sine (psinc) basis, with a grid size ($0.45a_o$), corresponding to a plane wave cut-off energy of 1020 eV. The PBE exchange-correlation functional was used with PBE OPIUM norm-conserving pseudopotentials.[79] The calculation was carried out in an implicit solvent using a dielectric of 4 to model induction effects.[48,80,81] The DDEC module implemented in ONETEP was used to partition the electron density and assign atom-centered point charges and atomic volumes.[47,82] The charges were assigned with a IH to ISA ratio of 0.02. The ESP error threshold, F_{thresh}, was set to 0.9025 kcal/mol. The additional charges are only added if the decrease in ESP error is larger than $F_{change} = 0.0625$ kcal/mol. The locations of the virtual sites were restricted using maximum distance cut-offs chosen by element, as virtual sites near the van der Waals radius can be detrimental. The cut-offs were defined as follows: 0.8 Å for N, 1 Å for O, S and F, and 1.5 Å for Cl and Br.

Pure Liquid Simulations

Pure liquid simulations were performed using OpenMM[83] with a custom non-bonded potential to describe the mixing rules and 1-4 interactions employed by the OPLS (and QUBE) FF. The required .xml files were generated using QUBEKit with extra sites included automatically using the local coordinate site construction function in OpenMM. All extra sites were modelled as virtual particles, and do not contribute bond and angle force field terms. For the construction of neighbor lists for 1-4 interactions, their only connection is made to the parent atom. A plot showing the agreement in single point energies calculated using the correction implemented in OpenMM and the BOSS software can be found in Figure S2. Instructions on how to perform the single point energy check for a new molecule using QUBEKit can be found at the Github (https://github.com/cole-group/QUBEKit/wiki) wiki page along with other examples and tutorials.

Simulations were performed in the isothermal-isobaric (NPT) ensemble at 1 atm and comprised 267 molecules in a periodic cubic box. Long-range electrostatic interactions were calculated using the Particle-Mesh-Ewald (PME) method,[84] with a 0.0005 tolerance error while also applying a long-range correction to the system energy. As in previous studies,[48,54] non-bonded interactions were truncated at distances based on molecular size (15 Å for molecules with 5 or more heavy atoms, 13 Å for 3–5 and 11 Å for fewer than 3) and smoothed over the last 0.5 Å. No long-range corrections to the Lennard-Jones energy were applied. Following minimization of the initial configuration, 3 ns simulations were run for each molecule using a 1 fs time step. The first nanosecond was treated as equilibration. Data showing the insensitivity of the computed liquid data to the choice of time step are shown in Table S3. The liquid and corresponding gas-phase simulations were run at 25°C or the molecule's boiling point if it was lower. The resulting densities and heats of vaporization were averaged over 2000 data points collected in the production part of the run. The heats of vaporization were computed using eq 8 in Ref. 85. Following their recommended protocol, we employed Langevin dynamics temperature regulation with a collision frequency of 5 ps^{-1}. The pressure was regulated using a Monte Carlo barostat as implemented in OpenMM. Examples of the scripts used for both the liquid and gas simulations along with input files for all molecules in the study can be found in the Supporting Information. The uncertainties were found to be less than 0.003 $\mathrm{g/cm}^3$ and 0.02 kcal/mol for densities and heats of vaporization respectively. Graphs showing the convergence of the properties with simulation time can also be found in Figures S4 and S5.

Free Energies of Hydration

Free energies of hydration were calculated using GROMACS[86] due to its ability to include extra sites during alchemical perturbation. All input files were generated using QUBEKit which writes OPLS FF style GROMACS .top and .gro files. The virtual sites were all constructed by hand using the simplest method available for each molecule, with a connection being added between the site and parent to again make the 1-4 interaction lists consistent with OpenMM and BOSS. Each molecule of the test set was annihilated from a cubic box containing approximately 1500 TIP4P water molecules using a two-step approach over 21 λ-windows, first turning of the charges followed by the L-J terms. The solute-solvent nonbonded interactions were switched off via coupling to the λ reaction parameter using soft-core potentials with settings $\alpha = 0.5$, $p = 1$ and $\sigma = 0.3$.[87] The charges were decoupled using λ values of (0.00 0.25 0.50 0.75 1.00) and van der Waals using λ values of (0.00 0.05 0.10 0.20 0.30 0.40 0.50 0.55 0.65 0.70 0.75 0.80 0.85 0.90 0.95 1.00). The simulations were again run in the NPT ensemble at 1 atm and 25°C. All solvent-solute and solvent-solvent non-bonded interactions were truncated at 10 Å and smoothed over the last 0.5 Å. PME was used with a long-range correction applied to the total energy and pressure. Each λ-window was run using Langevin dynamics and a two femtosecond time step with bonds involving hydrogen constrained using the LINCS algorithm.[88] The starting configurations at each λ-window were first minimized before being equilibrated twice. The first was a 100 ps run in the canonical ensemble (NVT) followed by a 200 ps run in the NPT ensemble. Finally, the production stage was run for 1 ns and the free energy of hydration was calculated using Bennett's acceptance ratio as implemented in the GROMACS BAR module.[89] All uncertainties for the calculations were found to be less than 0.3 kcal/mol.

Results and Discussion

Condensed Phase Properties

A common measure of the quality of FF parameters for use in biomolecular simulations is a comparison of the predicted condensed phase properties of molecules simulated using the FF with experiment. These properties, such as liquid density, the heat of vaporization and free energy of hydration, can be calculated routinely due to low sampling requirements, thus making FF inaccuracies the main contributor to any differences between the computed data and experiment. In this study, we have chosen a benchmark dataset comprising 109 small organic molecules, which are representative of the key functional groups commonly observed in biology and drug design. Importantly most of the molecules used in the set are also part of the training data used during the parametrization of many of the general transferable FFs mentioned, including the OPLS/1.14*CM1A-LBCC FF, which allows for direct comparison

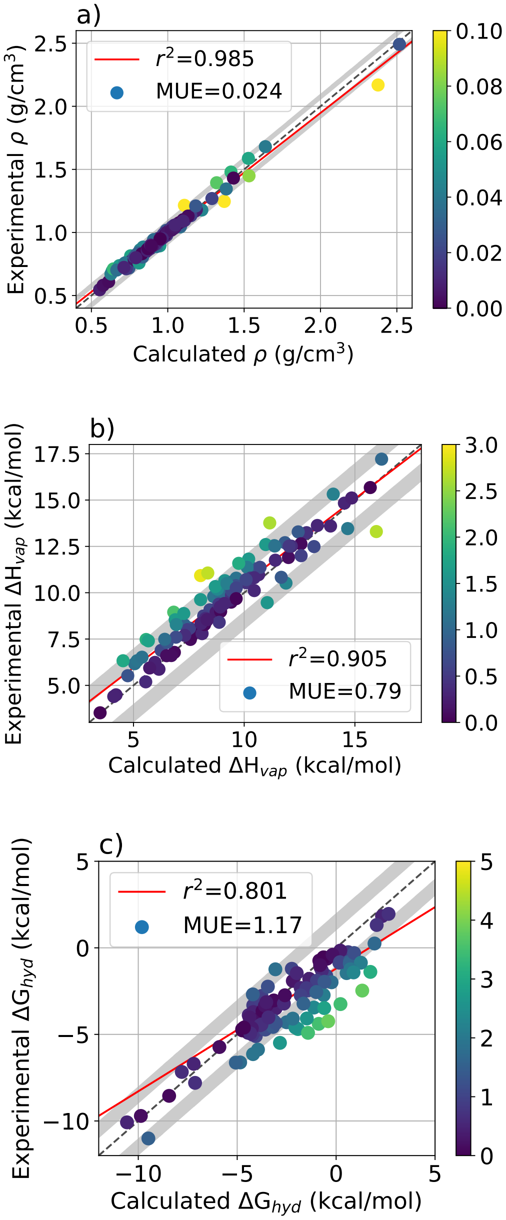

Figure 3: Force field liquid property metrics (a) liquid density, (b) heat of vaporization (c) free energy of hydration. Calculated for the organic molecule test set using QUBE FF parameters. MUE compared to experiment and r^2 correlation are also included.

Table 1: Mean unsigned errors between calculated liquid properties and experiment for various FF parameter sets.

Force field	ρ (g/cm^3)	ΔH_{vap} $(kcal/mol)$	ΔG_{hyd} $(kcal/mol)$
OPLS/1.14*CM1A[54]	0.024	1.40	1.26
GAFF/AM1-BCC[54]	0.039	1.31	0.94
OPLS/CM5[54]	0.024	1.06	0.94
OPLS/1.14*CM1A-LBCC[54]	0.024	1.40	0.61
DDEC/OPLS[48]	0.014	0.65	1.03
QUBE (this work)	0.024	0.79	1.17

of the FFs. Figure 3 shows the results of the condensed phase property calculations for the test set where experimental data are available, along with the correlations and mean unsigned errors (MUE), while Table 1 compares the latter with some examples of widely-used transferable FFs for the same test set.[7,48,54] The average errors in the density and heat of vaporization (0.024 g/cm^3 and 0.79 kcal/mol, respectively) indicate that QUBE performs extremely well in the prediction of pure liquid properties, that is despite only using eight fitting parameters in the derivation of non-bonded parameters (the van der Waals radii of the elements H, C, N, O, S, F, Cl, Br used in this study). Table S4 lists thirteen molecules the used for fitting and shows that removing them from the validation set has negligible effect on the analysis. Some of the outliers in the heat of vaporization predictions include interactions between aromatic rings, which may be due to the difficulty of describing van der Waals interactions using a simple r^{-6} interaction, which neglects higher-order dispersion and many-body effects. The general transferable force fields are of similar accuracy to QUBE, despite being extensively parametrized against data sets similar to these.

As we have found previously,[48] hydration free energies are more difficult to predict (MUE 1.17 kcal/mol). This could be due to limitations in the functional form, particularly the neglect of an explicit polarization term, in describing the transfer of a molecule between low dielectric (vacuum) and high dielectric (water) media, or the mixing rules used to compute L-J interactions. Though it should be noted that a MUE of 0.72 kcal/mol is reported using the OPLS3 FF on an expanded 239 molecule test set, which indicates that there is room for further improvement within the current FF functional form.[7] The largest outliers in Figure 3(c) are for apolar molecules with a low (less negative) free energy of hydration, for which QUBE under-estimates their solubility. This is particularly problematic again for molecules containing aromatic rings, and may indicate an imbalance between dispersive and electrostatic contributions to hydration when QUBE is used in combination with a standard transferable water model (TIP4P).

Table 2: The non-bonded parameters for the head group oxygen in 1-octanol are shown for a variety of FF and charge combinations. The LigParGen server was used to parameterize the OPLS variants, and Antechamber for GAFF with QUBE coming from this work.

Force field	charge	σ	ϵ
OPLS/1.14*CM1A	-0.588	3.120	0.170
OPLS/1.14*CM1A-LBCC	-0.687	3.120	0.170
GAFF/AM1-BCC	-0.598	1.721	0.210
QUBE	-0.673	3.129	0.127

Another potentially problematic group of compounds are aliphatic alcohols as we found the ten in our test set to have a relatively high MUE (1.27 kcal/mol) in hydration free energy. The poor description of alcohol groups was also previously found to be a trait of the OPLS/CM1A FF.[54,90] The charges assigned to the head group of 1-octanol by OPLS/CM1A are shown in Table 2. It has been suggested that scaled CM1A charges are too positive, resulting in the poor prediction of densities and heats of vaporization as shown in Table 3.[90] To tackle problematic groups such as these, the OPLS/1.14*CM1A-LBCC parametrization was developed which adds a systematic bond charge correction to various functional groups and was fit to better reproduce experimental free energies of hydration.[54] In the case of the aliphatic alcohols, the correction transfers a 0.1e$^-$ charge to the oxygen of the head group from the neighboring carbon atom as can be seen in Table 2. Thus with the same L-J parameters, the density, heat of vaporization and free energy of hydration are subsequently improved for 1-octanol, as shown in Table 3 along with the values obtained by the QUBE

FF. This same BCC was also found to reduce the MUE for the hydration free energy from 1.95 to 0.43 kcal/mol for 32 aliphatic alcohols in the development of the LBCC parameters.[54] Importantly the fitted correction scheme gives roughly the same charge as our AIM partitioning method which demonstrates the successful inclusion of polarization into our charges at the point of derivation rather than via subsequent corrections. We also observe similar σ parameters between the QUBE FF and OPLS, which is reassuring considering OPLS is extensively fit to reproduce liquid properties. While the ϵ values do differ noticeably, it has been found that liquid property predictions can be greatly improved with the systematic tuning of this parameter.[85] However, this would not be compatible with the philosophy of a QM derived FF, and future work will instead investigate modifications to the FF functional form.

Table 3: The liquid properties of 1-octanol predicted using different FF and charge parametrization methods are displayed and compared with experiment.

Force field	ρ (g/cm^3)	ΔH_{vap} $(kcal/mol)$	ΔG_{hyd} $(kcal/mol)$
OPLS/1.14*CM1A	0.807	15.201	-1.26
OPLS/1.14*CM1A-LBCC	0.809	16.038	-3.12
GAFF/AM1-BCC	0.834	20.354	-3.12
QUBE	0.793	16.206	-2.19
Experiment[90,91]	0.822	17.208	-4.09

Finally, it should be noted that there is an increase in the MUE of each of the properties computed using the QUBE FF compared with our original benchmark study (Table 1), which used AIM-derived non-bonded parameters in combination with OPLS bonded parameters (DDEC/OPLS).[48] This is likely the result of the expanded test set used here as on further inspection of the data concerning only the same molecules that were included in the original benchmark we find the MUEs to be 0.017 g/cm^3, 0.59 kcal/mol and 1.08 kcal/mol for the density, heat of vaporization and free energy of hydration respectively, which are very similar to the original values. We therefore, conclude that bonded parameters, while crucial to the conformational preferences of larger molecules, are not too important in the description of the liquid properties of small molecules.

With the inclusion of larger molecules and molecules that contain multiple functional groups, the increase in overall error of the liquid properties is to be expected if we consider the accuracy on a per functional group basis. This effect is exemplified by the case of o-chloroaniline, which has unsigned errors in ΔH_{vap} of 2.61 kcal/mol and in ΔG_{hyd} of 3.49 kcal/mol. By way of comparison, the smaller molecules aniline and chlorobenzene showed unsigned errors in ΔH_{vap} of 1.63 and 1.17 kcal/mol and in ΔG_{hyd} of 2.66 and 1.67 kcal/mol, respectively. This should be kept in mind when applying QUBE (and other force fields) to the study of, for example, absolute protein-ligand binding free energies for larger organic molecules containing multiple functional groups.

Bond, Angle and Dihedral Parameters

As discussed in the previous section, it appears that the bonded parameters have little effect on the accuracy of liquid properties. However, given the importance of torsional parameters in determining conformational preferences of larger molecules, and bond and angle parameters in modelling molecular vibrations, which are important for example in photochemistry applications, we examine the properties of the derived parameters here in more detail.

The first point to note is that by deriving bond and angle parameters directly from the QM Hessian matrix, there is no possibility of missing parameters in the QUBE FF. In contrast, even for this small test set, we found one missing bond parameter and six missing angle parameters using a standard transferable FF. The QUBE predicted values for these terms along with the OPLS atom types are shown in Tables S5 and S6. In practice, these parameters would be inferred from similar atom types or re-parameterized by the user, which may introduce inaccuracy. QUBE allows the user to rapidly and automatically derive all necessary parameters with no compromise in accuracy. In this study, the QUBE FF maintains a low mean percentage error in MM vibrational frequencies of 6.5% (MUE of 54 cm^{-1}), which is very similar to the values initially reported reaffirming the wide-scale applicability of the method.[34] We note that the modified Seminario method derives the force constants directly from the QM Hessian matrix with no information required about the torsional and non-bonded parameters. In practice, these components of the FF will also contribute to molecular vibrations. It appears that slight improvements in accuracy are achievable by fitting the full MM Hessian matrix to the QM Hessian.[30,44] For example, a MUE of 44 cm^{-1} is reported using the QMDFF on a set of 22 molecules.[30] Where high accuracy in molecular vibrations is key, for example in spectroscopic applications, it may be desirable to include coupling FF terms which account for off-diagonal terms in the Hessian matrix.[92] However, for our intended applications in computer-aided drug design, we favor the relative simplicity of the modified Seminario method.

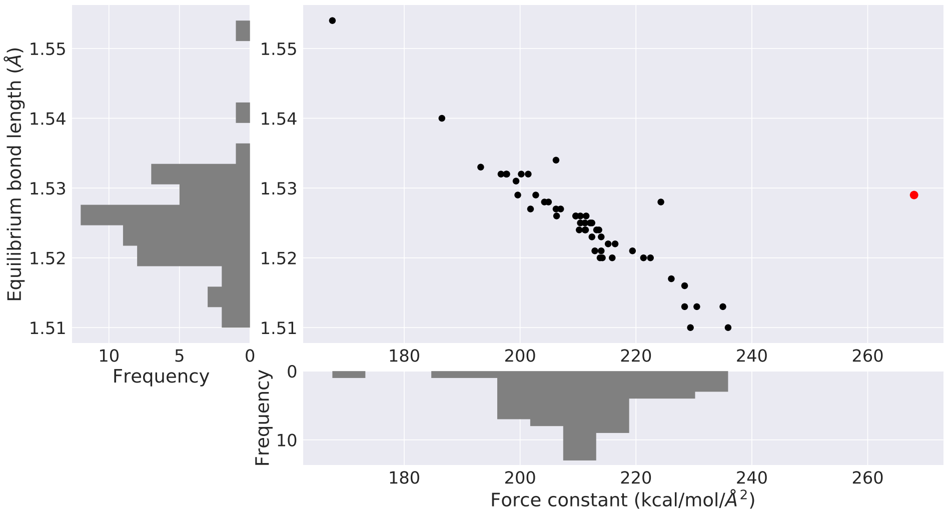

Figure 4: A common bond type is analyzed by comparing the QM predicted equilibrium bond length to the associated derived force constant of each molecule they appear in for the CT-CT bond type. The OPLS parameters are shown in red.

Given the widespread use of transferable bond and angle parameters, it is worth analyzing to what extent these parameters vary in our benchmark test set. Figure 4 plots the range of QUBE bond lengths and force constants for all atoms defined with CT-CT bond types in the test set, and compares them with the OPLS parameters. Further plots like this for all bonds and angles that are present in at least ten of the molecules in the test set can be found in Figures S7-S28. As reported previously,[34] the modified Seminario method gives bond-stretching force constants that are on average lower than their OPLS counterpart. The QUBE parameters typically span a range of around 0.05 Å and 100 kcal/mol/Å^2 for the bond length and force constant respectively, indicating that use of a single average, transferable value should not introduce significant error. Interestingly, there is a negative correlation between force constant and equilibrium bond length, supporting the use of bond length to infer force constants in early studies.[93] These results indicate that it may be possible to derive more explicit algorithms for 'learning' force field parameters directly from the molecular geometry. We also envisage QUBE parameters as providing a reasonable starting point for optimization if further fitting to QM potential energy surfaces is desired.[8]

Torsional parameters, like the bond and angle parameters, were derived separately for each molecule. Due to the use of virtual sites, we found that parameters were often not transferable between similar molecules, and those that were such as methyl group rotations remained close to the initial OPLS parameters. The overall accuracy of the torsional scan fitting was very good when regularization was used and only a handful of molecules with poor predicted energy surfaces required the setting to be switched off. A sample of torsion fitting data taken directly from the QUBEKit output can be found in Figures S29-S31, along with the overall error and regularization error bias where appropriate. We have also included the dihedral parameters for every molecule in the test set in the Supporting Information along with an analysis in which we have grouped the torsions together based on their OPLS atom types. We envisage these as forming the basis of a community-led library to be used to replace or speed up future fitting efforts.

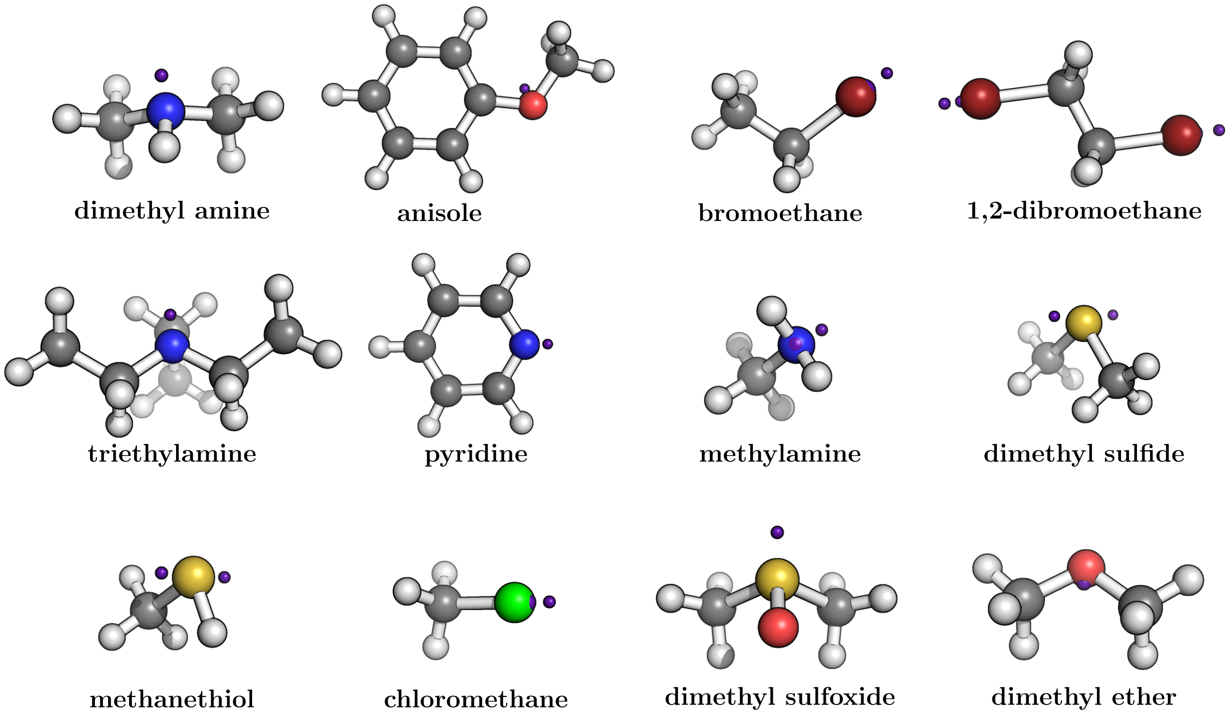

Figure 5: A selection of 12 molecules from the benchmark test set with their extra sites depicted as purple spheres. Charges and positions of the extra sites were derived from the partitioned atomic electron density.

Extra sites

To test the effect of the additional off-center point charges, the liquid properties for the benchmark test set were also calculated in the absence of extra sites. This led to a general worsening of the results with the MUEs becoming 0.023 g/cm^3, 0.85 kcal/mol and 1.51 kcal/-mol in the density, the heat of vaporization and free energy of hydration respectively (Figure S6). As expected, since it is governed mostly by Lennard-Jones interactions, the error in the density remained approximately constant. However, the decline in accuracy of the other properties indicates that modelling of anisotropy in electron density is required to accurately describe intermolecular interactions. This is consistent with the increasing use of virtual sites in multiple FFs.[7,94]

While there is no unique way to derive virtual site parameters, it would seem that deriving the parameters to minimize the error in ESP for an individual atom is effective. Figure 6 compares the ESP error around atoms before and after the addition of virtual sites. While

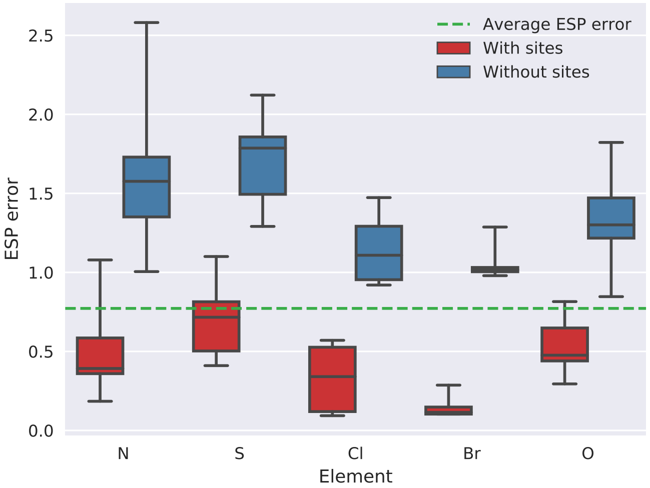

Figure 6: The average and range of the ESP error around each element for molecules in the test set before and after the addition of virtual sites. The dashed line represents the average error across all atoms in the benchmak set.

some residual error is to be expected given the simplicity of the FF functional form, the errors on these atoms displaying highly anisotropic electron density is now much closer to, and in many case below, the average ESP error across every atom in the benchmark set. Figure 5 shows a selection of molecules from the test set that required virtual sites, the rest of the derived site positions and corresponding charges can also be found in the Supporting Information. Here we can see that the derived positions are chemically intuitive, with σ-holes and lone-pairs well-represented. In total 50 of the 109 molecules in the test set required at least one virtual site, and on average a molecule whose functional group ESP error is initially above the chosen threshold requires 2.1 virtual sites. While this is more than is typical in molecular mechanics simulations, the computational cost of virtual sites in an MD simulation is small.[64] Furthermore, QUBEKit substantially simplifies the process for the user by deriving the virtual site parameters from QM and writing them to simulation-ready input files.

Some molecules with large ESP errors were not assigned off-center virtual sites. Chlorobenzene, for example, was found to have a large ESP error on the Cl atom just below the set threshold of 0.90 kcal/mol. However, the resulting liquid property predictions were not significantly affected (Table S9). Methanol was another example of a molecule that was not assigned virtual sites despite having an ESP error of 1.50 kcal/mol, which is above the threshold. After performing the grid search it was found that the addition of virtual sites did not substantially reduce the ESP error of the oxygen atom by the required amount F_{change}. This was the case for all aliphatic and aromatic alcohols in the test set which could also contribute to the poor performance of alcohols overall.

Test cases

While the molecules in the validation set represent many of the functional groups often used in drug design, they contain many fewer rotatable dihedral bonds and functional groups than a typical drug-like molecule. Thus, following previous work investigating the use of QM derived FF parameters we have used QUBEKit to derive a QUBE FF for 3-hydroxypropionic acid (3-HA).[71] The molecule shown in Figure 8 incorporates carboxyl and hydroxyl functional groups, has been identified as a potentially useful agent for organic synthesis and is also a surrogate for a typical fragment scaffold. QM-based fitting techniques have previously been used to derive the bonded parameters for the molecule from a series of single point energy calculations, with the L-J terms being taken from AMBER and the partial charges assigned according to the CHelpG scheme.[78] In addition, we have selected two further molecules from the FreeSolv database,[91] which allows us to compare computed hydration free energies with experiment for more challenging small drug-like molecules.[9] The two molecules, captan and bromacil (Figure 8), were selected due to the presence of halogens, and they therefore provide an additional test of the virtual site assignment procedure in QUBE.

Starting with the molecule 3-HA, Figure 7 compares the QUBE and OPLS force fields with QM single point calculations for a range of molecular geometries. Since we compute the bond and angle force constants in a one-off calculation directly from the QM Hessian matrix, with no iterative fitting, it is not obvious how accurate they will be in reproducing QM con-

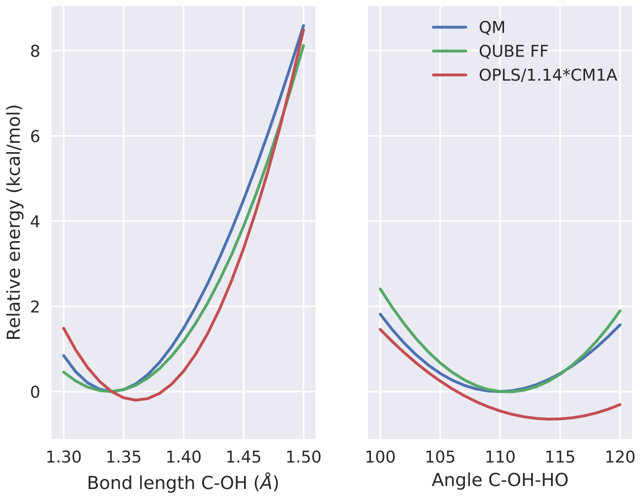

Figure 7: Comparison of the calculated relative single point energies using QM, OPLS and QUBE for C-OH bond-stretching and C-OH-HO angle-bending motions in 3-HA.

formational energetics when combined with the rest of the QUBE FF parameters. However, Figure 7 reveals that the QUBE FF reproduces extremely well, not only the QM minimum energy conformations, but also describes small changes in these same bond lengths and angles. This is also well replicated across all calculated vibrational modes for the molecule with an average percentage error of 6.7% compared to the QM vibrational frequencies.

Next, with the goal of evaluating the ability of QUBE to recreate intramolecular energetics including torsional rotations, separate liquid simulations of 3-HA, captan and bromacil solvated in boxes containing 1000 TIP4P water molecules were performed. We then extracted 500 conformations from each simulation and computed the relative single point energies of each snapshot of the molecule using OPLS, QUBE and QM (with the same DFT functional and basis sets as used for the parameter derivation). Figure 8 shows the correlation between the relative MM and QM energies for each of the three molecules. We note in making this comparison that, unlike QUBE, the OPLS FF was not parametrized against this QM model chemistry. Compared to OPLS, the correlation between MM and QM energetics is improved, and significantly QUBE does not sample any configurations that are lower in energy than the optimized QM structures. Figure S32 shows in more detail the fitting of QUBE torsion

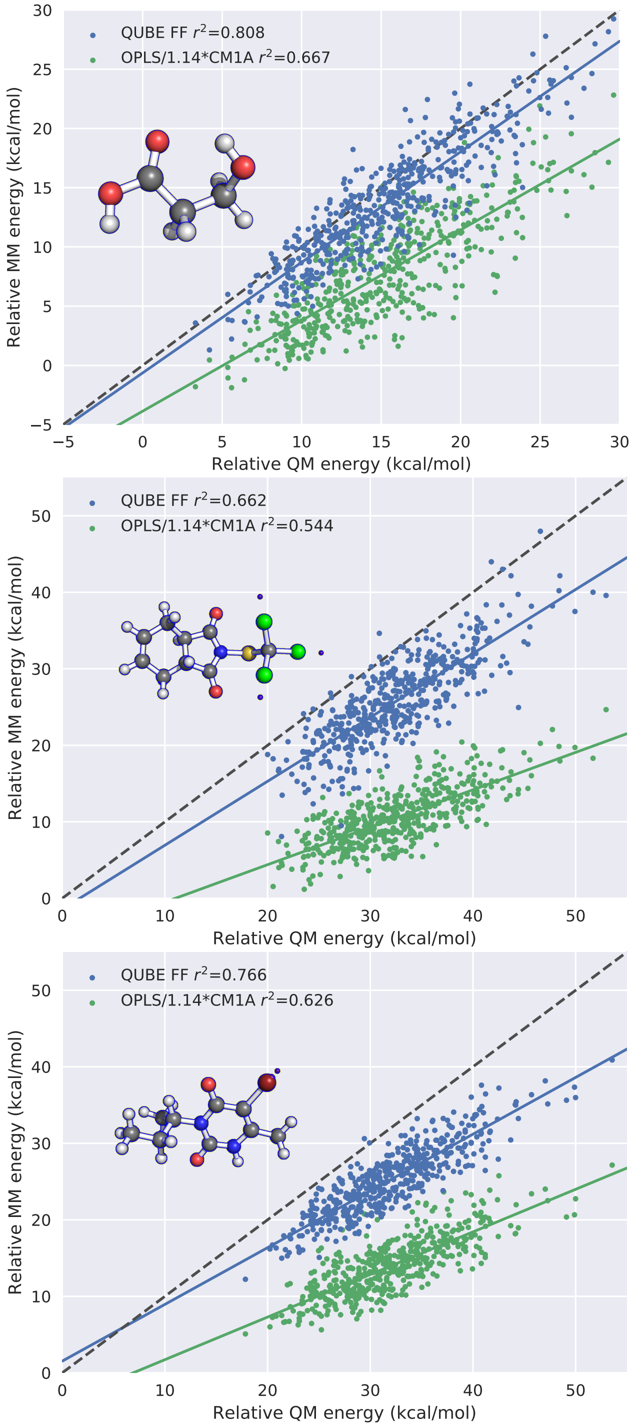

Figure 8: Comparison between the relative QM and MM energies using the QUBE FF and OPLS for 500 conformations extracted from a MD simulation of 3-HA (top), captan (center) and bromacil (bottom) which are shown as insets.

parameters to QM potential energy scans, as well as the dihedral angles sampled during MM dynamics in water. Encouragingly, despite the simple MM functional form used, and the fact that it is optimized for reproducing condensed phase properties, QUBE is not only able to reproduce the minimum energy structures, but also sample physically reasonable structures in liquid simulations, which is encouraging for future use in computer-aided drug design.

Table 4: The free energy of hydration predicted for two molecules from the FreeSolv database using the QUBE FF, compared to GAFF and experiment.[91]

	ΔG_{hyd} $(kcal/mol)$		
	QUBE	GAFF	Experiment
Captan	-5.48	-8.72	-9.01
Bromacil	-14.05	-14.50	-9.73

Finally, the free energies of hydration of captan and bromacil were calculated using the same protocol described earlier, and the results are shown in Table 4 alongside the experimental data and those computed using a GAFF parametrization.[91] The errors of around 4 kcal/mol in the QUBE FF are higher than those reported for the small molecule benchmark set, but consistent with expected cumulative errors in hydration free energy prediction. Nevertheless, improvements in accuracy are required, particularly for hydration free energy calculations, if QUBE is to be used in predictive computer-aided drug design. Future strategies along these lines are discussed in the next section.

Conclusions

With the spread of low-cost computing and access to automated software, it is becoming increasingly common for users to perform parameter set optimization prior to running molecular mechanics simulations. However, this optimization is typically used to supplement existing transferable force fields and is limited to the charge and torsional parameters, for which well-established protocols for fitting to QM data exist. On the other hand, QM derived force fields allow the user to obtain all (or most) of the force field parameters directly from *ab initio* calculations, but for these methods scaling to large molecules is problematic and there is no clear route to the simulation of, for example, biomolecular complexes. In this paper, we present the QUBEKit software for automated derivation of virtually all force field parameters required to model the dynamics of small organic molecules. QUBEKit is a python interface that brings together methods for charge and Lennard-Jones parameter derivation from atoms-in-molecule analysis of the QM electron density, and a method for deriving bond and angle force constants directly from the QM Hessian matrix. We also include a method for off-center virtual site derivation along with an automated implementation of a standard one-dimensional torsion fitting scheme.

Overall, we achieve mean unsigned errors of 0.024 g/cm^3, 0.79 kcal/mol and 1.17 kcal/-mol in the prediction of liquid densities, heats of vaporization and free energies of hydration for a benchmark set of 109 molecules, compared to experiment. This accuracy is particularly impressive compared to standard, transferable force fields when considering heats of vaporization and liquid densities. While competitive with many transferable FFs, there is substantial room for improvement in the prediction of hydration free energies. This is particularly highlighted when comparing the QUBE data in Table 1 with OPLS3, or when considering the larger molecules, captan and bromacil, in Table 4. Importantly, however, we emphasize that to describe all molecules in the benchmark data set, we have *only fit 8* parameters (the van der Waals radii of eight elements in vacuum) to experimental data (Table S4). This reduction in empiricism has two key advantages. Firstly, it has the potential to substantially simplify the FF fitting process, since the parameters come directly from QM and do not rely on extensive collection of experimental fitting data, which is time-consuming for small molecules, and is rarely done for larger molecules. Secondly, the ease of FF design presents the opportunity to derive new protocols, and move beyond the standard functional form of the FF whilst retaining the ability to derive non-bonded parameters for large molecules. Opportunities for FF improvement include: i) update of the atoms-in-molecule partitioning scheme,[95–99] ii) the introduction of more rigorous descriptions of van der Waals interactions,[100–102] iii) inclusion of explicit polarization, iv) a more accurate functional form for the short-range repulsion,[28,100] v) investigation of a QUBE-compatible water model[103] and vi) the investigation of Lennard-Jones combination rules. Such efforts would typically require significant re-fitting of the parameter libraries for transferable FFs. However, with the software infrastructure provided by QUBEKit, iterative improvements in the accuracy of the FF metrics presented here, particularly the hydration free energy, are envisaged.

One example of the update of our FF design protocol, is the addition in this paper of a method for off-center virtual site parameter derivation for the modelling of anisotropic electron density. Compared to our previous method,[48] the parameter derivation process is faster and more user-friendly. By deriving the virtual site charges and positions from the molecular symmetry and partitioned atomic electron density, we do not require any experimental data for fitting. Furthermore, since the bond, angle and Lennard-Jones parameter derivation methods are independent of the charge derivation, we can trivially add extra sites without substantially altering the force field. Notably, the mean unsigned error in the free energies of hydration of our benchmark set increases to 1.51 kcal/mol if virtual sites are not included. QUBEKit writes the virtual site positions in OpenMM .xml file format for ease-of-use.

In contrast to our previous work,[48] we have supplemented the atoms-in-molecule non-bonded parameters with molecule-specific bonded parameters derived from the QM Hessian matrix and torsional scans. In agreement with our previous study,[34] we showed that the so-called modified Seminario method is able to reproduce QM normal mode vibrational frequencies to high accuracy (6.5% here). Closer examination of bond and angle force field parameters for widely used atom types reveals that these parameters are reasonably transferable between closely-related molecules. Such analyses of more complex molecules could be used to identify problems with standard force fields where bonded parameters may require re-fitting or the inclusion of more atom types. In addition, we have shown that for three molecules, QM relative energies of an ensemble of structures are modelled reasonably well with the QUBE FF when combined with torsional fitting. It should be noted that torsional fitting is the major computational expense in QUBE (since it requires a constrained QM optimization at each torsion angle), and methods to reduce this expense are under investigation. In this regard, we have provided a library of all of the torsional parameters derived in this study, and these could be used as initial estimates for approximate dynamics, or as an initial guess in the fitting process. Improper torsional parameters are not derived in this study, and we have used those from the OPLS FF here. Potential future improvements include support for 2D torsion scans,[37] and the use of direct fitting to the Hessian matrix to allow derivation of stiff, harmonic torsional parameters and cross-terms to account for coupling between internal coordinates.[30,43,44,92] Such improvements are especially important in, for example, spectroscopic applications where a faithful representation of the QM intramolecular potential energy surface is crucial.[104,105]

We have provided with this paper the QUBEKit software toolkit, tutorials and data sets (https://github.com/cole-group/QUBEKit). This first version utilizes the BOSS molecular mechanics software,[77] and Gaussian09[61] and ONETEP[76] QM packages for parameter derivation. Simulation-ready files are output in OpenMM, Gromacs or BOSS format. Future work will widen the choice of available software, particularly for parameter derivation. Additional validation of QUBE against metrics such as condensed phase dielectric constants,[90] host-guest binding[31] and many more are envisaged, and we hope that QUBEKit will facilitate this process. In parallel, we are also releasing the QUBE protein force field,[49] which employs the same non-bonded parameter derivation techniques implemented in linear-scaling DFT software,[106] alongside a torsion library for the twenty naturally-occurring amino acids. Together these tools will allow users to derive compatible and accurate QUBE force fields for both proteins and small molecules for use in computer-aided drug design applications.

Acknowledgement

This research made use of the Rocket High Performance Computing service at Newcastle University. The authors acknowledge financial support from EPSRC grant EP/R010153/1 (DJC) and the EPSRC Centre for Doctoral Training in Computational Methods for Materials Science under grant EP/L015552/1 (AEAA).

Supporting Information Available

QUBEKit can be downloaded and installed from our Github page (https://github.com/cole-group/QUBEKit). Free atom reference data, details of molecules used during fitting, anisotropy workflow, single point BOSS and OpenMM energy comparison, QUBEKit workflow, N-(1-methylethyl)-2-propanamine and N,N-dimethylaniline liquid density and heat of vaporization property convergence, liquid density and thermodynamic property predictions excluding extra sites, QUBE predicted values for missing bond-stretching and angle-bending terms, QUBE predicted bond type analysis, QUBE predicted angle type analysis, some example dihedral fitting plots and chlorobenzene liquid property data. This material is available free of charge via the Internet at `http://pubs.acs.org/`.

References

(1) Mobley, D. L.; Klimovich, P. V. Perspective: Alchemical Free Energy Calculations for Drug Discovery. *J. Chem. Phys.* **2012**, *137*, 230901.

(2) Jorgensen, W. L. The Many Roles of Computation in Drug Discovery. *Science (New York, N.Y.)* **2004**, *303*, 1813–1818.

(3) De Vivo, M.; Masetti, M.; Bottegoni, G.; Cavalli, A. Role of Molecular Dynamics and Related Methods in Drug Discovery. *J. Med. Chem.* **2016**, *59*, 4035–4061.

(4) Wang, J.; Wang, W.; Kollman, P. A.; Case, D. A. Development and Testing of a General Amber Force Field. *J. Comput. Chem* **2004**, *25*, 1157–1174.

(5) Vanommeslaeghe, K.; Hatcher, E.; Acharya, C.; Kundu, S.; Zhong, S.; Shim, J.; Darian, E.; Guvench, O.; Lopes, P.; Vorobyov, I.; Mackerell, A. D. CHARMM General Force Field: A Force Field for Drug-Like Molecules Compatible with the CHARMM All-Atom Additive Biological Force Fields. *J. Comput. Chem.* **2010**, *31*, 671–690.

(6) Jorgensen, W. L.; Maxwell, D. S.; Tirado-Rives, J. Development and Testing of the OLPS All-Atom Force Field on Conformational Energetics and Properties of Organic Liquids. *J. Am. Chem. Soc.* **1996**, *118*, 11225–11236.

(7) Harder, E.; Damm, W.; Maple, J.; Wu, C.; Reboul, M.; Xiang, J. Y.; Wang, L.; Lupyan, D.; Dahlgren, M. K.; Knight, J. L.; Kaus, J. W.; Cerutti, D. S.; Krilov, G.; Jorgensen, W. L.; Abel, R.; Friesner, R. A. OPLS3: A Force Field Providing Broad Coverage of Drug-like Small Molecules and Proteins. *J. Chem. Theory Comput.* **2016**, *12*, 281–296.

(8) Wang, L. P.; Martinez, T. J.; Pande, V. S. Building Force Fields: An Automatic, Systematic, and Reproducible Approach. *J. Phys. Chem. Lett.* **2014**, *5*, 1885–1891.

(9) Mobley, D. L.; Bannan, C. C.; Rizzi, A.; Bayly, C. I.; Chodera, J. D.; Lim, V. T.; Lim, N. M.; Beauchamp, K. A.; Slochower, D. R.; Shirts, M. R.; Gilson, M. K.; Eastman, P. K. Escaping Atom Types in Force Fields Using Direct Chemical Perception. *J. Chem. Theory Comput.* **2018**, *14*, 6076–6092, PMID: 30351006.

(10) Jorgensen, W. L.; Jensen, K. P.; Alexandrova, A. N. Polarization Effects for Hydrogen-Bonded Complexes of Substituted Phenols with Water and Chloride Ion. *J. Chem. Theory Comput.* **2007**, *3*, 1987–1992.

(11) Jakalian, A.; Bush, B. L.; Jack, D. B.; Bayly, C. I. Fast, Efficient Generation of High-

Quality Atomic Charges. AM1-BCC Model: I. Method. *J. Comput. Chem.* **2000**, *21*, 132–146.

(12) Jakalian, A.; Jack, D. B.; Bayly, C. I. Fast, Efficient Generation of High-Quality Atomic Charges. AM1-BCC Model: II. Parameterization and Validation. *J. Comput. Chem.* **2002**, *23*, 1623–1641.

(13) Storer, J. W.; Giesen, D. J.; Cramer, C. J.; Truhlar, D. G. Class IV Charge Models: A New Semiempirical Approach in Quantum Chemistry. *J. Comput. Aided Mol. Des.* **1995**, *9*, 87–110.

(14) Tkatchenko, A.; Scheffler, M. Accurate Molecular van der Waals Interactions from Ground-State Electron Density and Free-Atom Reference data. *Phys. Rev. Lett.* **2009**, *102*, 6–9.

(15) Tkatchenko, A.; DiStasio Jr, R. A.; Car, R.; Scheffler, M. Accurate and Efficient Method for Many-Body van der Waals Interactions. *Phy. Rev. Lett.* **2012**, *108*, 236402.

(16) Clementi, E.; Corongiu, G.; Ranghino, G. Analytical Potentials from ab Initio Computations for the Interaction Between Biomolecules. VII. Polar Amino Acids and Conclusions. *J. Chem. Phys.* **1981**, *74*, 578–588.

(17) Lie, G. C.; Clementi, E. Study of the Structure of Molecular Complexes. XII. Structure of Liquid Water Obtained by Monte Carlo Simulation with the Hartree–Fock Potential Corrected by Inclusion of Dispersion Forces. *J. Chem. Phys.* **1975**, *62*, 2195–2199.

(18) Kistenmacher, H.; Popkie, H.; Clementi, E.; Watts, R. O. Study of the Structure of Molecular Complexes. VII. Effect of Correlation Energy Corrections to the Hartree-Fock Water–Water Potential on Monte Carlo Simulations of Liquid water. *J. Chem. Phys.* **1974**, *60*, 4455–4465.

(19) Linse, P.; Engström, S.; Jönsson, B. Molecular Dynamics Simulation of Liquid and Solid Benzene. *Chem. Phys. Lett.* **1985**, *115*, 95–100.

(20) Karlstroem, G.; Linse, P.; Wallqvist, A.; Joensson, B. Intermolecular Potentials for the Water-Benzene and the Benzene-Benzene Systems Calculated in an ab Initio SCFCI Approximation. *J. Am. Chem. Soc.* **1983**, *105*, 3777–3782.

(21) Cacelli, I.; Cinacchi, G.; Prampolini, G.; Tani, A. Computer Simulation of Solid and Liquid Benzene with an Atomistic Interaction Potential Derived from ab Initio Calculations. *J. Am. Chem. Soc.* **2004**, *126*, 14278–14286.

(22) Prampolini, G.; Livotto, P. R.; Cacelli, I. Accuracy of Quantum Mechanically Derived Force-Fields Parameterized from Dispersion-Corrected DFT data: The Benzene Dimer as a Prototype for Aromatic Interactions. *J. Chem. Theory Comput.* **2015**, *11*, 5182–5196.

(23) Greff da Silveira, L.; Jacobs, M.; Prampolini, G.; Livotto, P. R.; Cacelli, I. Development and Validation of Quantum Mechanically Derived Force-Fields: Thermodynamic, Structural, and Vibrational Properties of Aromatic Heterocycles. *J. Chem. Theory Comput.* **2018**, *14*, 4884–4900.

(24) Waldher, B.; Kuta, J.; Chen, S.; Henson, N.; Clark, A. E. ForceFit: A Code to Fit Classical Force Fields to Quantum Mechanical Potential Energy Surfaces. *J. Comp. Chem.* **2010**, *31*, 2307–2316.

(25) Cacelli, I.; Lami, C. F.; Prampolini, G. Force-Field Modeling through Quantum Mechanical Calculations: Molecular Dynamics Simulations of a Nematogenic Molecule in its Condensed Phases. *J. Comp. Chem.* **2009**, *30*, 366–378.

(26) Xu, P.; Guidez, E. B.; Bertoni, C.; Gordon, M. S. Perspective: Ab Initio Force Field Methods Derived from Quantum Mechanics. *J. Chem. Phys.* **2018**, *148*, 090901.

(27) McDaniel, J. G.; Schmidt, J. Physically-Motivated Force Fields from Symmetry-Adapted Perturbation Theory. *J. Phys. Chem. A.* **2013**, *117*, 2053–2066.

(28) Van Vleet, M. J.; Misquitta, A. J.; Stone, A. J.; Schmidt, J. R. Beyond Born-Mayer: Improved Models for Short-Range Repulsion in ab Initio Force Fields. *J. Chem. Theory Comput.* **2016**, *12*, 3851–3870.

(29) Vandenbrande, S.; Waroquier, M.; Speybroeck, V. V.; Verstraelen, T. The Monomer Electron Density Force Field (MEDFF): A Physically Inspired Model for Noncovalent Interactions. *J. Chem. Theory Comput.* **2016**, *13*, 161–179.

(30) Grimme, S. A General Quantum Mechanically Derived Force Field (QMDFF) for Molecules and Condensed Phase Simulations. *J. Chem. Theory Comput.* **2014**, *10*, 4497–4514.

(31) Yin, J.; Henriksen, N. M.; Slochower, D. R.; Shirts, M. R.; Chiu, M. W.; Mobley, D. L.; Gilson, M. K. Overview of the SAMPL5 Host–Guest Challenge: Are We Doing Better? *J. Comput. Aided Mol. Des.* **2017**, *31*, 1–19.

(32) Mobley, D. L.; Gilson, M. K. Predicting Binding Free Energies: Frontiers and Benchmarks. *Annu. Rev. Biophys.* **2017**, *46*, 531–558.

(33) Steinbrecher, T. B.; Dahlgren, M.; Cappel, D.; Lin, T.; Wang, L.; Krilov, G.; Abel, R.; Friesner, R.; Sherman, W. Accurate Binding Free Energy Predictions in Fragment Optimization. *J. Chem. Inf. Model.* **2015**, *55*, 2411–2420.

(34) Allen, A. E. A.; Payne, M. C.; Cole, D. J. Harmonic Force Constants for Molecular Mechanics Force Fields via Hessian Matrix Projection. *J. Chem. Theory Comput.* **2018**, *14*, 274–281.

(35) Seminario, J. M. Calculation of Intramolecular Force Fields from Second-Derivative Tensors. *Int. J. Quantum Chem.* **1996**, *60*, 1271–1277.

(36) Hagler, A. Quantum Derivative Fitting and Biomolecular Force Fields: Functional Form, Coupling Terms, Charge Flux, Nonbond Anharmonicity, and Individual Dihedral Potentials. *J. Chem. Theory Comput.* **2015**, *11*, 5555–5572.

(37) Wang, L.-P.; McKiernan, K. A.; Gomes, J.; Beauchamp, K. A.; Head-Gordon, T.; Rice, J. E.; Swope, W. C.; Martínez, T. J.; Pande, V. S. Building a more Predictive Protein Force Field: A Systematic and Reproducible Route to AMBER-FB15. *J. Phys. Chem. B.* **2017**, *121*, 4023–4039.

(38) Verstraelen, T.; Van Neck, D.; Ayers, P.; Van Speybroeck, V.; Waroquier, M. The Gradient Curves Method: An Improved Strategy for the Derivation of Molecular Mechanics Valence Force Fields from ab Initio Data. *J. Chem. Theory Comput.* **2007**, *3*, 1420–1434.

(39) Boulanger, E.; Huang, L.; Rupakheti, C.; MacKerell, A. D.; Roux, B. Optimized Lennard-Jones Parameters for Druglike Small Molecules. *J. Chem. Theory Comput.* **2018**, *14*, 3121–3131.

(40) Burger, S. K.; Lacasse, M.; Verstraelen, T.; Drewry, J.; Gunning, P.; Ayers, P. W. Automated Parametrization of AMBER Force Field Terms from Vibrational Analysis with a Focus on Functionalizing Dinuclear Zinc (II) Scaffolds. *J. Chem. Theory Comput.* **2012**, *8*, 554–562.

(41) Dasgupta, S.; Goddard III, W. A. Hessian-Biased Force Fields from Combining Theory and Experiment. *J. Chem. Phys.* **1989**, *90*, 7207–7215.

(42) Dasgupta, S.; Brameld, K. A.; Fan, C.-F.; Goddard III, W. A. ab Initio Derived Spectroscopic Quality Force Fields for Molecular Modeling and Dynamics. *Spectrochimica Acta Part A: Mol. Biomol. Spectrosc.* **1997**, *53*, 1347–1363.

(43) Cacelli, I.; Prampolini, G. Parametrization and Validation of Intramolecular Force

Fields Derived from DFT Calculations. *J. Chem. Theory Comput.* **2007**, *3*, 1803–1817.

(44) Barone, V.; Cacelli, I.; De Mitri, N.; Licari, D.; Monti, S.; Prampolini, G. Joyce and Ulysses: Integrated and User-Friendly Tools for the Parameterization of Intramolecular Force Fields from Quantum Mechanical data. *Phys. Chem. Chem. Phys.* **2013**, *15*, 3736–3751.

(45) Hu, L.; Ryde, U. Comparison of Methods to Obtain Force-Field Parameters for Metal Sites. *J. Chem. Theory Comput.* **2011**, *7*, 2452–2463.

(46) Wang, R.; Ozhgibesov, M.; Hirao, H. Partial Hessian Fitting for Determining Force Constant Parameters in Molecular Mechanics. *J. Comput. Chem.* **2016**, 2349–2359.

(47) Lee, L. P.; Cole, D. J.; Skylaris, C. K.; Jorgensen, W. L.; Payne, M. C. Polarized Protein-Specific Charges from Atoms-In-Molecule Electron Density Partitioning. *J. Chem. Theory Comput.* **2013**, *9*, 2981–2991.

(48) Cole, D. J.; Vilseck, J. Z.; Tirado-Rives, J.; Payne, M. C.; Jorgensen, W. L. Biomolecular Force Field Parameterization via Atoms-in-Molecule Electron Density Partitioning. *J. Chem. Theory Comput.* **2016**, *12*, 2312–2323.

(49) Allen, A. E. A.; Robertson, M. J.; Payne, M. C.; Cole, D. J. Introducing QUBE: Quantum Mechanical Bespoke Force Fields for Protein Simulations. **2019**, 10.26434/chemrxiv.7565222.v1.

(50) Zheng, S.; Tang, Q.; He, J.; Du, S.; Xu, S.; Wang, C.; Xu, Y.; Lin, F. VFFDT: A New Software for Preparing AMBER Force Field Parameters for Metal-Containing Molecular Systems. *J. Chem. Inf. Model.* **2016**, *56*, 811–818.

(51) Li, P.; Merz, K. M. MCPB.py: A Python Based Metal Center Parameter Builder. *J. Chem. Inf. Model.* **2016**, *56*, 599–604.

(52) Dewar, M. J. S.; Zoebisch, E. G.; Healy, E. F.; Stewart, J. J. P. Development and use of Quantum Mechanical Molecular Models. 76. AM1: a New General Purpose Quantum Mechanical Molecular Model. *J. Am. Chem. Soc.* **1985**, *107*, 3902–3909.

(53) Dodda, L. S.; De Vaca, I. C.; Tirado-Rives, J.; Jorgensen, W. L. LigParGen Web Server: An Automatic OPLS-AA Parameter Generator for Organic Ligands. *Nucleic Acids Res.* **2017**, *45*, 331–336.

(54) Dodda, L. S.; Vilseck, J. Z.; Tirado-Rives, J.; Jorgensen, W. L. Localized Bond Charge Corrected CM1A Charges for Condensed-Phase Simulations Corrected CM1A Charges for Condensed-Phase Simulations. *J. Phys. Chem. B* **2017**, *121*, 3864–3870.

(55) Jorgensen, W. L.; Tirado-Rives, J. Potential Energy Functions for Atomic-Level Simulations of Water and Organic and Biomolecular Systems. *Proc. Natl. Acad. Sci. U. S. A.* **2005**, *102*, 6665–6670.

(56) Damm, W.; Frontera, A.; Rives, J. T.; Jorgensen, W. L. OPLS All-Atom Force Field for Carbohydrates. *J. Comp. Chem.* **1997**, *18*, 1955–1970.

(57) Manz, T. A.; Sholl, D. S. Chemically Meaningful Atomic Charges That Reproduce the Electrostatic Potential in Periodic and Nonperiodic Materials. *J. Chem. Theory Comput.* **2010**, *6*, 2455–2468.

(58) Manz, T. A.; Sholl, D. S. Improved Atoms-in-Molecule Charge Partitioning Functional for Simultaneously Reproducing the Electrostatic Potential and Chemical States in Periodic and Nonperiodic Materials. *J. Chem. Theory Comput.* **2012**, *8*, 2844–2867.

(59) Dodda, L. S.; Vilseck, J. Z.; Cutrona, K. J.; Jorgensen, W. L. Evaluation of CM5 Charges for Nonaqueous Condensed-Phase Modeling. *J. Chem. Theory Comput.* **2015**, *11*, 4273–4282.

(60) Chu, X.; Dalgarno, A. Linear Response Time-Dependent Density Functional Theory for van der Waals Coefficients. *J. Chem. Phys.* **2004**, *121*, 4083–4088.

(61) Frisch, M. J.; Trucks, G. W.; Schlegel, H. B.; Scuseria, G. E.; Robb, M. A.; Cheeseman, J. R.; Scalmani, G.; Barone, V.; Mennucci, B.; Petersson, G. A.; Nakatsuji, H.; Caricato, M.; Li, X.; Hratchian, H. P.; Izmaylov, A. F.; Bloino, J.; Zheng, G.; Sonnenberg, J. L.; Hada, M.; Ehara, M.; Toyota, K.; Fukuda, R.; Hasegawa, J.; Ishida, M.; Nakajima, T.; Honda, Y.; Kitao, O.; Nakai, H.; Vreven, T.; Montgomery, J. A., Jr.; Peralta, J. E.; Ogliaro, F.; Bearpark, M.; Heyd, J. J.; Brothers, E.; Kudin, K. N.; Staroverov, V. N.; Kobayashi, R.; Normand, J.; Raghavachari, K.; Rendell, A.; Burant, J. C.; Iyengar, S. S.; Tomasi, J.; Cossi, M.; Rega, N.; Millam, J. M.; Klene, M.; Knox, J. E.; Cross, J. B.; Bakken, V.; Adamo, C.; Jaramillo, J.; Gomperts, R.; Stratmann, R. E.; Yazyev, O.; Austin, A. J.; Cammi, R.; Pomelli, C.; Ochterski, J. W.; Martin, R. L.; Morokuma, K.; Zakrzewski, V. G.; Voth, G. A.; Salvador, P.; Dannenberg, J. J.; Dapprich, S.; Daniels, A. D.; Farkas, .; Foresman, J. B.; Ortiz, J. V.; Cioslowski, J.; Fox, D. J. Gaussian09 Revision E.01. Gaussian Inc. Wallingford CT 2009.

(62) Manz, T. A.; Gabaldon Limas, N. Chargemol Program for Performing DDEC Analysis. Available from http://ddec.sourceforge.net (accessed September 2014).

(63) Kramer, C.; Spinn, A.; Liedl, K. R. Charge Anisotropy: Where Atomic Multipoles Matter Most. *J. Chem. Theory Comput.* **2014**, *10*, 4488–4496.

(64) Unke, O. T.; Devereux, M.; Meuwly, M. Minimal Distributed Charges: Multipolar Quality at the Cost of Point Charge Electrostatics. *J. Chem. Phys.* **2017**, *147*, 161712.

(65) Jorgensen, W. L.; Chandrasekhar, J.; Madura, J. D.; Impey, R. W.; Klein, M. L. Comparison of Simple Potential Functions for Simulating Liquid Water. *J. Chem. Phys.* **1983**, *79*, 926–935.

(66) Yan, X. C.; Robertson, M. J.; Tirado-Rives, J.; Jorgensen, W. L. Improved Description of Sulfur Charge Anisotropy in OPLS Force Fields: Model Development and Parameterization. *J. Phys. Chem. B* **2017**, *121*, 6626–6636.

(67) Macchiagodena, M.; Mancini, G.; Pagliai, M.; Barone, V. Accurate Prediction of Bulk Properties in Hydrogen Bonded Liquids: Amides as Case Studies. *Phys. Chem. Chem. Phys.* **2016**, *18*, 25342–25354.

(68) Macchiagodena, M.; Mancini, G.; Pagliai, M.; Del Frate, G.; Barone, V. Fine-Tuning of Atomic Point Charges: Classical Simulations of Pyridine in Different Environments. *Chem. Phys. Lett.* **2017**, *677*, 120–126.

(69) Dubay, K. H.; Hall, M. L.; Hughes, T. F.; Wu, C.; Reichman, D. R.; Friesner, R. A. Accurate Force Field Development for Modeling Conjugated Polymers. *J. Chem. Theory Comput.* **2012**, *8*, 4556–4569.

(70) Robertson, M. J.; Tirado-Rives, J.; Jorgensen, W. L. Improved Peptide and Protein Torsional Energetics with the OPLS-AA Force Field. *J. Chem. Theory Comput.* **2015**, *11*, 3499–3509.

(71) Chen, S.; Yi, S.; Gao, W.; Zuo, C.; Hu, Z. Force Field Development for Organic Molecules: Modifying Dihedral and 1-n Pair Interaction Parameters. *J. Comput. Chem.* **2015**, *36*, 376–384.

(72) Wildman, J.; Repiščák, P.; Paterson, M. J.; Galbraith, I. General Force-Field Parametrization Scheme for Molecular Dynamics Simulations of Conjugated Materials in Solution. *J. Chem. Theory Comput.* **2016**, *12*, 3813–3824.

(73) Dahlgren, M. K.; Schyman, P.; Tirado-Rives, J.; Jorgensen, W. L. Characterization of Biaryl Torsional Energetics and its Treatment in OPLS All-Atom Force Fields. *J. Chem. Inf. Model.* **2013**, *53*, 1191–1199.

(74) Zgarbová, M.; Rosnik, A. M.; Luque, F. J.; Curutchet, C.; Jurečka, P. Transferability and Additivity of Dihedral Parameters in Polarizable and Nonpolarizable Empirical Force Fields. *J. Comput. Chem.* **2015**, *36*, 1874–1884.

(75) Vanommeslaeghe, K.; Yang, M.; Mackerell, A. D. Robustness in the Fitting of Molecular Mechanics Parameters. *J. Comput. Chem.* **2015**, *36*, 1083–1101.

(76) Skylaris, C. K.; Haynes, P. D.; Mostofi, A. A.; Payne, M. C. Introducing ONETEP: Linear-Scaling Density Functional Simulations on Parallel Computers. *J. Chem. Phys.* **2005**, *122*.

(77) Jorgensen, W. L.; Tirado-Rives, J. Molecular Modeling of Organic and Biomolecular Systems using BOSS and MCPRO. *J. Comput. Chem.* **2005**, *26*, 1689–1700.

(78) Chai, J. D.; Head-Gordon, M. Long-Range Corrected Hybrid Density Functionals with Damped Atom-Atom Dispersion Corrections. *Phys. Chem. Chem. Phys.* **2008**, *10*, 6615–6620.

(79) Perdew, J. P.; Burke, K.; Ernzerhof, M. Generalized Gradient Approximation Made Simple. *Phys. Rev. Lett.* **1996**, *77*, 3865–3868.

(80) Womack, J. C.; Anton, L.; Dziedzic, J.; Hasnip, P. J.; Probert, M. I.; Skylaris, C. K. DL-MG: A Parallel Multigrid Poisson and Poisson-Boltzmann Solver for Electronic Structure Calculations in Vacuum and Solution. *J. Chem. Theory Comput.* **2018**, *14*, 1412–1432.

(81) Dziedzic, J.; Helal, H. H.; Skylaris, C. K.; Mostofi, A. A.; Payne, M. C. Minimal Parameter Implicit Solvent Model for ab Initio Electronic-Structure Calculations. *Europhys. Lett.* **2011**, *95*.

(82) Lee, L. P.; Gabaldon Limas, N.; Cole, D. J.; Payne, M. C.; Skylaris, C.-K.; Manz, T. A.

Expanding the Scope of Density Derived Electrostatic and Chemical Charge Partitioning to Thousands of Atoms. *J. Chem. Theory Comput.* **2014**, *10*, 5377–5390.

(83) Eastman, P.; Swails, J.; Chodera, J. D.; Mcgibbon, R. T.; Zhao, Y.; Beauchamp, K. A.; Simmonett, A. C.; Harrigan, M. P.; Brooks, B. R.; Pande, V. S. OpenMM 7 : Rapid Development of High Performance Algorithms for Molecular Dynamics. *PLoS Comput. Biol.* **2017**, *13*, e1005659.

(84) Essmann, U.; Perera, L.; Berkowitz, M. L.; Darden, T.; Lee, H.; Pedersen, L. G. A Smooth Particle Mesh Ewald Method A Smooth Particle Mesh Ewald Method. *J. Chem Phys.* **1995**, 8577–8593.

(85) Wang, J.; Hou, T. Application of Molecular Dynamics Simulations in Molecular Property Prediction. 1. Density and Heat of Vaporization. *J. Chem. Theory Comput.* **2011**, *7*, 2151–2165.

(86) Abraham, M. J.; Murtola, T.; Schulz, R.; Páll, S.; Smith, J. C.; Hess, B.; Lindahl, E. Gromacs: High Performance Molecular Simulations through Multi-Level Parallelism from Laptops to Supercomputers. *SoftwareX* **2015**, *1-2*, 19–25.

(87) Beutler, T. C.; Mark, A. E.; van Schaik, R. C.; Gerber, P. R.; van Gunsteren, W. F. Avoiding Singularities and Numerical Instabilities in Free Energy Calculations Based on Molecular Simulations. *Chem. Phys. Lett.* **1994**, *222*, 529–539.

(88) Hess, B.; Bekker, H.; Berendsen, H. J. C.; Johannes, G. E. M. F. LINCS: a Linear Constraint Solver for Molecular Simulations. *J. Comput. Chem.* **1997**, *18*, 1463–1472.

(89) Bennett, C. H. Efficient Estimation of Free Energy Differences from Monte Carlo data. *J. Comput. Phys.* **1976**, *22*, 245–268.

(90) Caleman, C.; Van Maaren, P. J.; Hong, M.; Hub, J. S.; Costa, L. T.; Van Der Spoel, D. Force Field Benchmark of Organic Liquids: Density, Enthalpy of Vaporization, Heat

Capacities, Surface Tension, Isothermal Compressibility, Volumetric Expansion Coefficient, and Dielectric Constant. *J. Chem. Theory Comput.* **2012**, *8*, 61–74.

(91) Mobley, D. L.; Guthrie, J. P. FreeSolv: a Database of Experimental and Calculated Hydration Free Energies, with Input Files. *J. Comput.-Aided Mol. Des.* **2014**, *28*, 711–720.

(92) Cerezo, J.; Prampolini, G.; Cacelli, I. Developing Accurate Intramolecular Force Fields for Conjugated Systems through Explicit Coupling Terms. *Theor. Chem. Acc.* **2018**, *137*, 80.

(93) Weiner, S. J.; Kollman, P. A.; Case, D. A.; Singh, U. C.; Ghio, C.; Alagona, G.; Profeta, S.; Weiner, P. A New Force Field for Molecular Mechanical Simulation of Nucleic Acids and Proteins. *J. Am. Chem. Soc.* **1984**, *106*, 765–784.

(94) Doherty, B.; Zhong, X.; Acevedo, O. Virtual Site OPLS Force Field for Imidazolium-Based Ionic Liquids. *J. Phys. Chem. B* **2018**, *122*, 2962–2974.

(95) Manz, T. A.; Limas, N. G. Introducing DDEC6 Atomic Population Analysis: Part 1. Charge Partitioning Theory and Methodology. *RSC Advances* **2016**, *6*, 47771–47801.

(96) Limas, N. G.; Manz, T. A. Introducing DDEC6 Atomic Population Analysis: Part 2. Computed Results for a Wide Range of Periodic and Nonperiodic Materials. *RSC Advances* **2016**, *6*, 45727–45747.

(97) Manz, T. A. Introducing DDEC6 Atomic Population Analysis: Part 3. Comprehensive Method to Compute Bond Orders. *RSC Advances* **2017**, *7*, 45552–45581.

(98) Limas, N. G.; Manz, T. A. Introducing DDEC6 Atomic Population Analysis: Part 4. Efficient Parallel Computation of Net Atomic Charges, Atomic Spin Moments, Bond Orders, and more. *RSC Advances* **2018**, *8*, 2678–2707.

(99) Manz, T.; Chen, T.; Cole, D. J.; Limas, N. G.; Fiszbein, B. Introducing DDEC6 Atomic Population Analysis: Part 5. New Method to Compute Polarizabilities and Dispersion Coefficients. **2018**, 10.26434/chemrxiv.7205693.v1.

(100) Stone, A. J. Intermolecular Potentials. *J. Science* **2008**, *321*, 787–788.

(101) Walters, E. T.; Mohebifar, M.; Johnson, E. R.; Rowley, C. N. Evaluating the London Dispersion Coefficients of Protein Force Fields Using the Exchange-Hole Dipole Moment Model. *J. Phys. Chem. B* **2018**, *122*, 6690–6701.

(102) Misquitta, A. J.; Stone, A. J. ISA-Pol: Distributed Polarizabilities and Dispersion Models from a Basis-Space Implementation of the Iterated Stockholder Atoms Procedure. **2018**, arxiv:1806.06737.

(103) Piana, S.; Donchev, A. G.; Robustelli, P.; Shaw, D. E. Water Dispersion Interactions Strongly Influence Simulated Structural Properties of Disordered Protein States. *J. Phys. Chem. B.* **2015**, *119*, 5113–5123.

(104) Kraner, S.; Prampolini, G.; Cuniberti, G. Exciton Binding Energy in Molecular Triads. *J. Phys. Chem. C.* **2017**, *121*, 17088–17095.

(105) Andreussi, O.; Prandi, I. G.; Campetella, M.; Prampolini, G.; Mennucci, B. Classical Force Fields Tailored for QM Applications: Is It Really a Feasible Strategy? *J. Chem. Theory Comput.* **2017**, *13*, 4636–4648.

(106) Cole, D. J.; Hine, N. D. M. Applications of Large-Scale Density Functional Theory in Biology. *J. Phys. Condens. Matter* **2016**, *28*, 393001.

Graphical TOC Entry

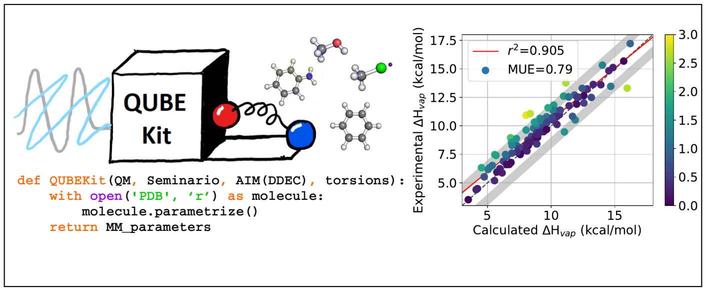

```
def QUBEKit(QM, Seminario, AIM(DDEC), torsions):
    with open('PDB', ‘r’) as molecule:
        molecule.parametrize()
    return MM_parameters
```